AN ABSTRACT OF THE THESIS OF

Alireza Mostafizi for the degree of Master of Science in Civil Engineering presented on May 19, 2016.

Title: Agent-based Tsunami Evacuation Model: Life Safety and Network Resilience

Abstract approved: _____

Haizhong Wang

Natural disasters could result in unnecessary loss of life and disproportionate suffering to families and communities if evacuation plans are not in place or understood by the public. In the Pacific Northwest, a magnitude 9.0 earthquake and tsunami from the Cascadia Subduction Zone (CSZ) represents one of the most pressing natural disasters with an astonishing high 7%-12% chance of occurrence by 2060. The destructive nature of earthquakes and the subsequent near-field tsunami, and also the retrofitting challenges of infrastructure network motivates us to accurately model the tsunami evacuation to reduce the number of fatalities. This thesis presents an agent-based multi-modal near-field tsunami evacuation modeling framework in Netlogo.

The goals of this study are two folded. The first objective is to investigate how (1) decision time, (2) choice of modes of transportation (i.e., walking and automobile), and in general (3) different variables involved in the evacuation scenario (e.g., walking speed and driving speed) impact the estimation of casualties. Using the city of Seaside, Oregon as a study site, which is one of the most vulnerable cities on the Oregon coast, different evacuation scenarios are included in the model to assess the impact of parameters involved on the mortality rate of the tsunami event. The results show that (1) evacuation mode choice strongly influences the expected number of casualties; (2) the mortality rate is strongly correlated with decision-making time (τ); and (3) the mortality rate is sensitive

to the variations in walking speed of the evacuee population.

Secondly, this study extends the agent-based modeling framework to assess the transportation network vulnerability in Seaside, OR, under unplanned disruptions (i.e., bridge failures) due to the Cascadia Subduction Zone earthquake initiating a near-field tsunami on the coast of State of Oregon. The criticality of each link in the entire network is evaluated iteratively by connecting the impacts of link failures on the resultant mortality rate. After assessing all the links, an innovative method is developed to identify the most critical links within the network. Further assessment is conducted on the identified critical links to formulate an optimal network retrofitting plan to minimize the mortality rate considering the limited amount of resources. The framework has been tested on the transportation network of city of Seaside, OR, and the results show that the critical links are not necessarily the bridges in the network. Therefore, the identification of the critical links requires a systematic assessment of the entire transportation network, and furthermore, minimizing the mortality rate necessitates the logical use of available resources.

Agent-based Tsunami Evacuation Model: Life Safety and Network Resilience

by

Alireza Mostafizi

A THESIS

submitted to

Oregon State University

in partial fulfillment of
the requirements for the
degree of

Master of Science

Presented May 19, 2016
Commencement June 2016

Master of Science thesis of Alireza Mostafizi presented on May 19, 2016

APPROVED:

Major Professor, representing Civil Engineering

Head of the School of Civil & Construction Engineering

Dean of the Graduate School

I understand that my thesis will become part of the permanent collection of Oregon State University libraries. My signature below authorizes release of my thesis to any reader upon request.

Alireza Mostafizi, Author

ACKNOWLEDGEMENTS

I would like to express my sincere appreciation for the contribution of my advisor, Dr. Haizhong Wang in this work. I would like to thank him for his constant support and guidance that paved my way throughout this research. Joyful and fruitful collaboration with him has been a blessing over the past two years.

I am also grateful to my committee members, Dr. Dan Cox and Dr. Lori A. Cramer. I would have not been able to come this far without their guidance. In addition, the contribution of Dr. Cox and Dr. Hyoungsu Park in generating the tsunami inundation component of the model and providing the relevant material is highly appreciated. I would like to also acknowledge the contribution of Dr. Cramer in modeling the social aspects of tsunami evacuation and her valuable input in this regard. Further, I would like to thank her for her thorough edits of my manuscript.

I would like to acknowledge the funding support from the Oregon Sea Grant program through the project "Building resilient coastal communities: A social assessment of mobile technology for tsunami evacuation planning," and also from National Science Foundation through the project "An Integrated Social Science and Agent-based Modeling Approach to Improve Life Safety from Near-field Tsunami Hazards."

At the end, I would like to thank my family. Their unconditional love and support accompanied me through every step of my life, and I will always be grateful of having them beside me. This work is dedicated to them.

TABLE OF CONTENTS

TABLE OF CONTENTS (Continued)

LIST OF FIGURES

LIST OF FIGURES (Continued)

LIST OF TABLES

AGENT-BASED TSUNAMI EVACUATION MODEL: LIFE SAFETY AND NETWORK RESILIENCE

1. INTRODUCTION

The Pacific Northwest region is highly prone to a near-field Tsunami initiated from a mega-thrust earthquake (Goldfinger et al., 2012). Near-field tsunamis are expected to come onshore within 20 to 40 minutes as opposed to far-field tsunamis or other natural disasters which may take hours, or in some cases, days, to affect the area of interest, which allows longer lead time to issue warning and evacuation notices (NRC, 2011). The low preparation time severely adds complexity to the evacuation scenario, and even a well-established agency as Pacific Tsunami Warning Center (PTWC) might not be able to provide sufficient warning time for the event (Katada et al., 2006).

1.1. Problem Definition

In 2004, the Indian Ocean earthquake and tsunami resulted in a total death of more than 230,000 people; and in 2011, Tohoku earthquake and tsunami resulted in over 16,000 fatalities. These casualties are due to a wide variety of reasons including people's inability to evacuate the damage zones and areas subject to tsunami inundation. However, since it is practically unrealistic to build all structures in a way that resists tsunami forces, evacuation tends to be the best and most effective way to reduce fatalities. Tsunami evacuation modeling is a newly developing tool to evaluate the impacts of heterogeneous decision-making on survivability and effectiveness of evacuation plans to set land use

and construction policy in areas subjected to devastation. Although tsunami evacuation models exist, the existing models are essentially static and there has been little effort to assess the behavioral aspects included in the models such as milling time and evacuation mode choice.

Other than loss of life, damages to Infrastructure network represents another issue. The large-scale evacuation represents a complex system for the transport operation and planning to minimize casualties, including the potential damages to critical infrastructure and communication systems from the earthquake (Lammel, 2011). Therefore, evacuation itself, and the required infrastructure, needs to be studied more than it has been in order to achieve effective emergency evacuations.

Furthermore, transportation network is one of the most critical components of the civil infrastructure system susceptible to natural hazards such as earthquakes. The performance of the transportation network is essential to emergency responses and to recovery activities following an immediate earthquake. Depending on the magnitude and duration of an earthquake, the transportation network typically suffers from certain levels of mobility losses (due to link failures) caused by either landslide, rockfalls, or bridge failure (OSSPAC, 2013). Bridges in transportation networks, specifically, are "lifeline" infrastructures and vital to the operation of the network. However, they are continuously deteriorating over time and are particularly vulnerable to seismic hazards (Chang et al., 2012). It is critical that bridges retain their traffic-carrying capacities after a devastating earthquake so that people can efficiently evacuate to safer areas. Retrofitting existing bridges is a widely accepted and relatively economical way to enhance bridges' performance against earthquakes and mitigate their functional loss (Chang et al., 2012). Nevertheless, it is neither practical nor economical to retrofit all existing bridges due to budget constraints. In addition, the level of retrofitting is of great significance. Therefore, it is vital to prioritize the bridges' retrofitting with an appropriate strategy. Besides

bridges, maintenance of some of the transportation links might also be of significance. The criticality of any specific link or bridge is reinforced by the lack of alternative links in an evacuation scenario. Since life safety is the most important measure to evaluate the success of a near-field tsunami evacuation, exploring the effect of network disruption through evacuation mortality would provide an innovative and straightforward perspective to prioritize a retrofitting strategy in a way to minimize the mortality rate considering the limited resources.

1.2. Objectives

Unknowns and complexities of evacuation scenarios, both from socio-psychological and engineering perspectives necessitates further investigation of the impact of different elements (e.g., mode choice, milling time, and evacuation speed) on the estimation of casualties in a multi-modal tsunami evacuation. Therefore, this research aims to model the evacuee's decision-making behavior during the near-field tsunami evacuation event which can lead to a better comprehension of the evacuation process and the factors affecting the mortality rate of the scenario (e.g., whether to evacuate or not? Which mode of transportation? Which route to take?). According to a survey conducted by Mas et al. (2011) regarding Tohoku tsunami in 2011, 57% of the interviewees evacuated immediately after the earthquake while 37% had delayed their evacuation. A general evacuation model may provide a regional perspective, however, site-specific case studies are useful for emergency planning at those specific locations (Wood and Schmidtlein, 2013). Thus, this study uses the city of Seaside, Oregon as a case for the multi-modal agent-based evacuation model, where the sizable population is constantly threatened by near-field tsunamis (Wood and Schmidtlein, 2012).

In addition, assessment of transportation network component in the evacuation pro-

cess and devising a framework to systematically recognize, identify, and retrofit the critical network components is another objective of this research. Unplanned transportation network disruptions, including local link disruptions (e.g. bridge failures) by a combined earthquake and tsunami hazard is a phenomenon that is caused by most of the natural hazards. This research integrates the transportation network disruption uncertainties into a multi-modal agent-based evacuation model to assess the impacts of disruptions considering evacuee's choice of modes (i.e. car, walking on foot) and their life safety from a network-wide perspective. An innovative agent-based modeling framework is used to identify and classify the criticality of network links, based on their failure impact on the mortality rate of the evacuation, and further, the framework is used to devise the optimal retrofitting plan for the critical links of the network.

Research results will enlighten policy-makers and city planners on, for one, the behavior of the evacuation and the impacts of the factors involved in any kind of evacuation scenarios on the mortality rate of the disaster, in order to optimize the evacuation strategies. Secondly, results inform officials on how link disruptions or bridge failures can affect the evacuees' rerouting decision-making behavior, and ultimately, the efficiency of the evacuation scenario, in order to devise a logical retrofitting plan for critical links of the transportation network and rationally allocate the limited retrofitting resources. As a case study, an optimal retrofitting plan has been identified to minimize the fatalities considering the limited resources for the city of Seaside, OR.

1.3. Thesis Organization

This thesis begins by presenting a thorough literature review on related topics in section 2. Section 3. introduces the agent-based simulation framework and the methodology to achieve the desired expectations, along with the description of the study site.

Section 4. presents the first objective of this study, which involves a detailed explanation of the evacuation behavior and the impacts of the factors involved. Moreover, the distribution of casualties are presented using travel trajectories of evacuees in section 4.2.. The second objective is presented in Section 5. which includes the approach of marking the critical links in the network and the detailed retrofitting plan for the identified critical links. Finally, following the results, this manuscript concludes with section 6. which summarizes the research and discusses the major findings from the case study, along with description of the challenges ahead in agent-based tsunami evacuation modeling and simulation, and the modeling of complex interactions between agents (i.e., pedestrian and car interactions) that would arise for a multi-hazard scenario for the Cascadia Subduction Zone.

2. LITERATURE REVIEW

Due to the life-threatening risk posed by various disasters, evacuation is likely to be called to ensure the life safety. However, the unique warning time across the hazards create challenges for efficient evacuation. Figure 2.1 presents five distinct hazard groups whose warning time increase from seconds (i.e., earthquake) to hours (i.e., hurricane) as is revealed in the hazard length and time scales. Evacuation plans for earthquakes and building fires generally occur over short time scales, seconds to a few minutes, and evacuees are on foot to shelter in place or nearby. For example, in the case of an earthquake, an evacuee might take refuge under a desk within a few seconds of feeling the strong shaking of the building. On the other hand, evacuations from hurricanes often have several hours to days of advanced warning, and evacuees rely on vehicles to seek shelter several miles away beyond the hazard zone. Extensive research has been done regarding the evacuation modeling for many different kinds of natural hazards over the past decades, as Figure 2.2 represents a few highlighted ones.

Near-field tsunamis present a complex case of multi-modal evacuation because the tsunami arrives within several minutes, typically 20 to 40 minutes, of the earthquake and can travel several kilometers inland. Therefore, transportation evacuation modes, may be multi-modal rather than a single mode, and evacuees may be faced with choices of sheltering nearby (vis-a-vis vertical evacuation) on foot or to travel outside of the inundation zone by car. The multi-modal state of evacuation in these cases necessitates extensive research on the traffic flow modeling and crowd dynamics in emergencies. In the following, a comprehensive literature review is presented on current evacuation modeling techniques, agent-based modeling methods, social vulnerability in disasters, and post-disaster network disruption.

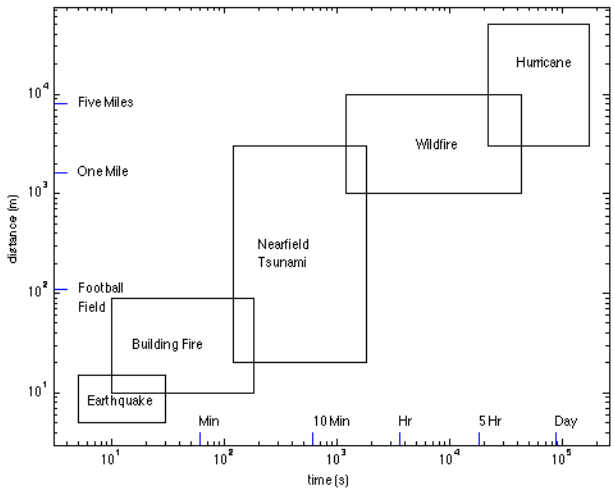

FIGURE 2.1: Evacuation from evacuee's perspective for different hazards (Wang et al., 2015)

2.1. Evacuation Modeling

A mass disaster episode is the result of an interaction between two highly complex, dynamic and generally hard-to-predict phenomena: a human community and a hazard (Assaf, 2011). Due to the complexity of human behaviors, the system can rarely be described as mathematical equations. Various techniques have been proposed to model this complex system. The existing efforts are summarized into the following categories (Almeida et al., 2013; Santos and Aguirre, 2004):

Flow-based modeling: Flow-based models are called macroscopic models, and use the density of nodes in continuous flows. The underlying logic is derived from an analogy between the fluid and particle motions. Their characteristics are predefined; thus, all the particles behave in the same way, which is the major drawback of this approach. One example is EVACNET4 (Santos and Aguirre, 2004).

Cellular Automata: In this type of model, space is discretized, which differentiates it

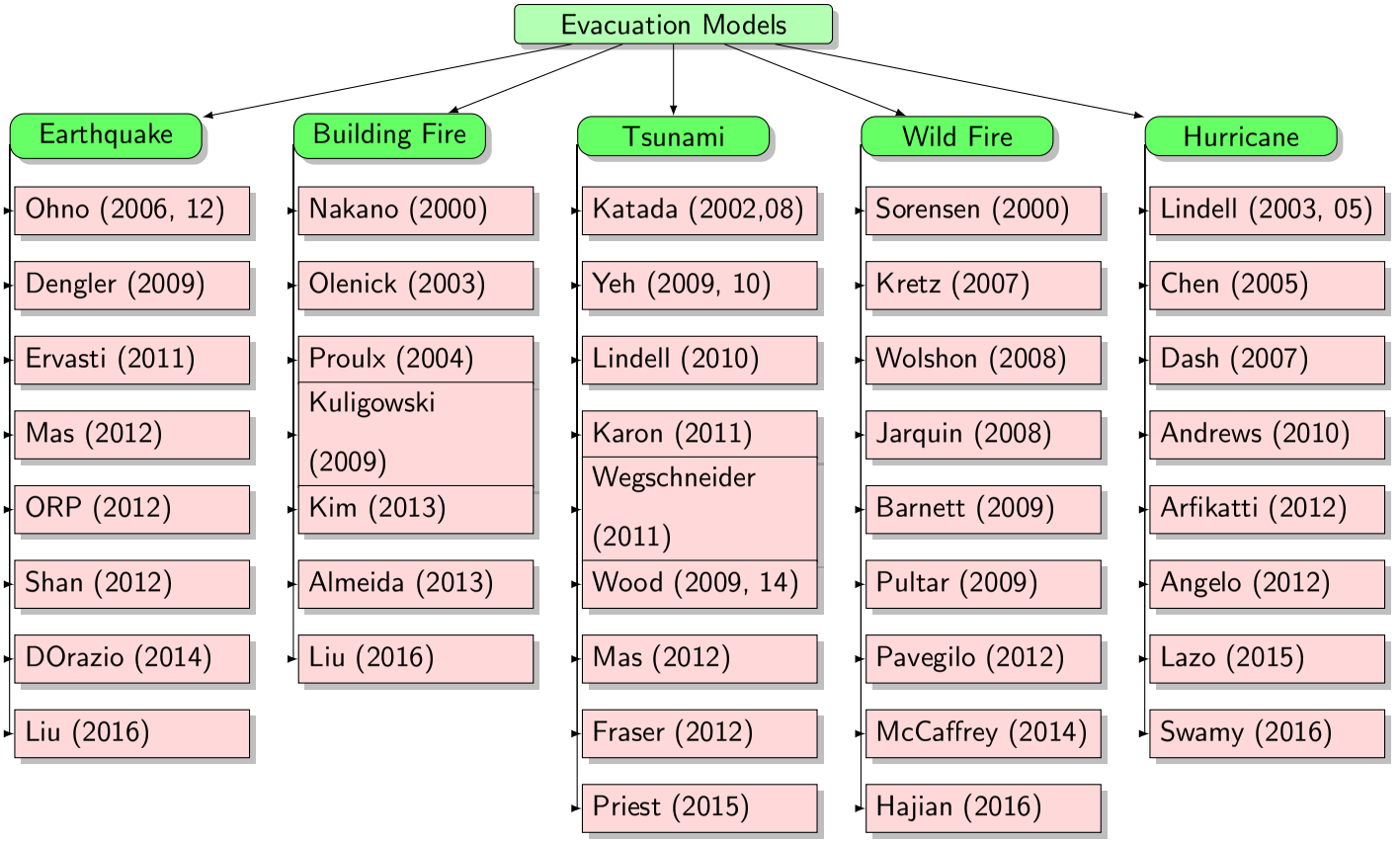

FIGURE 2.2: Summary of highlighted evacuation models for varying hazards (the warning time increases from left to right)

from all other modeling techniques (Santos and Aguirre, 2004). A matrix is created to plot areas in a two-dimensional array. In the simulation, the occupants move from one position to one of the adjacent nodes in a predefined time frame. Microscopic and macroscopic analysis are both permitted. This is easy to implement but fails to replicate the complex movement of people, especially the two-dimensional nature of pedestrian movements. Furthermore, due to the grid-shaped network, it is rather hard to depict the different speeds and interaction between people. One example is EGRESS (Pan et al., 2007).

Agent-based modeling: Multi-Agent System (MAS) approach is deemed the most realistic solution due to its capability to model each individual with unique characteristics and interactions with the surrounding environment. Representative examples are SIMULEX (Santos and Aguirre, 2004), the latest version of EXODUS (Santos and Aguirre, 2004), and PedGo (Jafari et al., 2003).

Other than the methods mentioned above, in the past decades, approaches such as static networks (shortest path, minimum cost network flow, or quickest path), dynamic networks, and traffic assignment have been widely employed to model the evacuation scenario (Hamacher and Tjandra, 2002). Wood and Schmidtlein (2012) used a least-cost-distance (LCD) model to assess pedestrian-evacuation potential from CSZ-related tsunamis in the US Pacific Northwest. LCD models focus on evacuation landscape features (Wood and Schmidtlein, 2013) and use geographic information systems (GIS) to find the shortest path to safe spots from hazard zones (Wood and Schmidtlein, 2012). A typical example of evacuation simulation based on static concepts is MASSVAC (Hobeika et al., 1994.). An integrated GIS-based simulator framework, which employed the shortest-path algorithm, was developed by Katada et al. to improve evacuation efficiency (Katada et al., 2006). Chalmet et al. (1982) suggested using the dynamic network to model the circumstance that many occupants evacuated in minimum time. Sheffi et al. (1982.)

proposed the NETVAC model for simulating the traffic pattern under an emergency evacuation scenario. Dynamic traffic assignment (DTA) has also been utilized for emergency evacuation modeling (Kwon and Pitt, 2005). Lovs (1998) presented the way-finding problem in emergency evacuation using various models in a mathematical setting, providing various models. Figure 2.3 highlights some of the relevant evacuation traffic simulation models (Pel et al., 2012).

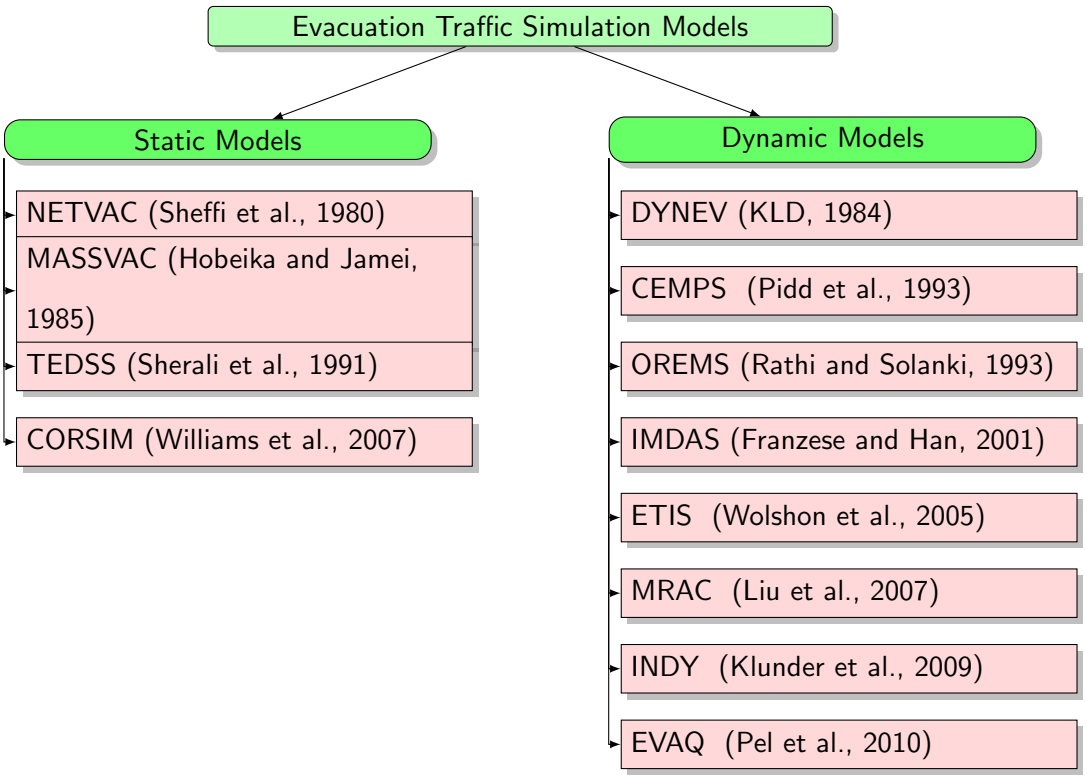

FIGURE 2.3: Evacuation traffic simulation models

However, these methods contain weaknesses that prevent them from realistically replicating real world situations. For example, shortest path solution does not consider congestion effects, which tend to underestimate the travel times, and the shortcoming of static assignment is that it does not possess the consideration of the time-of-day dynamics (Lammel, 2011); they neglect central behavioral aspects like panic or herding behavior as well (Lammel, 2011). Traditional methods lack the capacity to describe the

individuals' decision-making behavior in that circumstance, nor fully incorporate the potential interaction effects between evacuees. Human behavior is highly complex, and is the most difficult aspect of the evacuation process and hard to model in mathematical equations (Mas et al., 2011). The desired approach for the evacuation problem is an iterative learning method, which could be improved by agent-based modeling and simulation (ABMS) (Lammel, 2011). ABMS is situated to offer meaningful insights into the mechanisms and preconditions for decision making processes under pressure and panic.

2.2. Agent-based Modeling

An agent-based modeling and simulation (ABMS) is an object oriented modeling technique to simulate the interactions and actions of the autonomous decision-making entities, assessing the effect as a whole to capture the emergent phenomena. Hundreds of agents, who are repeatedly interacting over time, operate concurrently to investigate the connection between the macro and micro level individual's behavior (Mas et al., 2011). Each agent individually assesses its situation and makes an evacuation decision on the basis of a set of rules (Dawson et al., 2011). The ABM has demonstrated it can provide insights that are not available from other methods and captures both the natural and human system dynamics (Dawson et al., 2011). The benefits of ABM over other modeling techniques can be highlighted in three statements (Bonabeau, 2002): (1) ABM captures emergent phenomena; (2) ABM provides a natural description of a system; and (3) ABM is flexible. The ABM technique has already been employed in several studies. For example, Chen and Zhan (2006) introduced an agent-based technique to model the traffic flow and investigate collective behavior of evacuees. Nagarajan et al. (2012) developed a multi-agent simulation model and deployed it in a warning information dissemination study. Mas et al. (2012, 2011) proposed an evacuation model integrated with a numerical

simulation of a tsunami and a casualty estimation evaluation to study life safety considering evacuees' decision-making regarding the evacuation start time. Liu et al. (2009) formulated a dynamic route choice model in a multi-agent system when considering group evacuation. Uno and Kashiyama (2008) proposed a multi-agent emergency evacuation simulation system. Dawson et al. (2011) adopted a dynamic agent-based model to manage flood incidents.

Although recent research efforts have begun using agent-based modeling frameworks for hurricanes and coastal community tsunami evacuation (Mas et al., 2011), the existing tsunami evacuation research models typically assumes 100% pedestrian walking with little consideration of other modes of transportation such as automobiles or bicycles. This is despite recent work where it was observed that a large number of evacuees left from low-topography areas by car (Mas et al., 2011).

2.3. Network Disruption

The frequency and intensity of natural disasters have increased (Newkirk, 2001) over past decades and the network disruption is an inevitable consequence. Along with the frequent occurrences of natural disasters such as earthquakes, tsunamis, and floods, the lifeline infrastructure resilience and recovery is one of most significant and challenging topics in the community emergency preparedness. Thus, network disruption is central to lifeline emergency response and recovery analysis. In addition, evacuation demand is compressed into a relatively short time span. It is critical to investigate the transportation network under duress to ensure life safety (Balakrishna et al., 2008).

Network disruptions refer to a series of events that change the regular flow of traffic on one or more roadway facilities. Generally, network disruptions are classified as planned and unplanned events. Planned disruptions include traffic congestion or road or ramp

closures to accommodate work zones along a freeway segment or bridge section and transit strikes etc. (Konduri et al., 2013; Zhu and Levinson, 2012). Unplanned disruptions include natural disasters (e.g., tsunamis, earthquakes, floods, landslides, hurricanes), terrorist attacks (e.g. September 11), infrastructure failures (e.g. I-35W bridge collapse), severe accidents, etc. (Zhu and Levinson, 2012; Jenelius et al., 2010). Network disruptions lead to a drop in capacity on the roadway segment where the incident occurs and result in delays, built up queues, and spill-backs on to surrounding areas in the network (Konduri et al., 2013). A partial decrease or complete loss of capacity on a road or bridge link can result in travel time increase and changes in travel behavior through congestion and queues. Empirical evidence shows that a majority of unplanned transport network disruptions are followed by "a time-on the order of days or weeks-of uncertainty, learning and adaptation for the travelers" (Jenelius et al., 2010). If the network disruption lasts for a long time, the traffic eventually reaches a new equilibrium, where travelers collect sufficient information and change their travel behaviors accordingly. In such cases, unplanned disruptions have similar impacts to traffic as planned disruptions, as people are more informed and have time to change travel decisions; most commonly are changes to departure time and route choice (Jenelius et al., 2010). However, the immediacy of an evacuation would leave no room for adaptation. Various approaches have been proposed to model the network disruptions, including static analysis (Earnest, 2011), equilibrium analysis (Miller et al., 1999), weighted network model (Earnest, 2011), disruption index (Murray-Tuite and Mahmassani, 2005; Rahimian and Mcneil, 2012), agent-based models (Earnest, 2011), damage index (Rahimian and Mcneil, 2012), probability model (Chang et al., 2012), and travel time analysis (Bocchini and Frangopol, 2010).

When it comes to emergency response or disaster evacuation, a system performance metric is required to assess the serviceability of a road network and compare the effectiveness resulting from different intervention or mitigation projects. Such system metrics

for road networks can be divided into three categories: (1) connectivity, (2) travel delay cost, and (3) network flow capacity (Chang et al., 2012). Connectivity relies highly on the connectedness of a transportation network. However, it ignores traffic systems' capacities, travel time, and trip length. Travel delay cost has been widely adopted to assess the seismic risk of transportation systems (Kiremidjian et al., 2007). Nevertheless, it is heavily dependent on origin-destination (OD) demand matrices. Network flow capacity metric falls in between: it evaluates the serviceability of transportation networks under specifically determined seismic damage and does not require detailed OD demand information or traveler behavior to compute the travel delay cost. It serves better to evaluate the emergency serviceability of a transportation network in terms of immediate population evacuation. Berdica (2002) defined the vulnerability as "a susceptibility to incidents that can result in considerable reductions in road network serviceability." The serviceability of a link is defined as "the possibility to use that link during a given time period." However, previous research did not examine the availability of alternative links for a specific link in the transportation network.

Moreover, it is vital to know the details of the impacts of the system disruption; for example, where events are most likely to happen, and where impacts would be the most severe (Jenelius and Mattsson, 2012). The desire to better understand the impacts of network disruptions has led to a rich body of research. This literature can be classified into two categories, (1) measuring the change of activity-travel behavior in response to network perturbation and user information provision and (2) tool development for simulating network disruptions and evaluating various policies and solutions to alleviate the impacts of network disruptions (Konduri et al., 2013). Zhu et al. (2010) investigated the impact of the collapse of the I-35W bridge over the Mississippi River on regional traffic flow and travel behavior patterns. Akiyama et al. (2012) proposed a probability assessment of bridge performance by estimating bridge failure likelihood through bridge fragility curves.

As Murray-Tuite (2007) stated, "before planning network improvement, they should examine the degree to which the disruption of a link, or set of links, will influence network connectivity." Network connectivity plays a significant part in the performance of the network, especially during an evacuation. However, the connectivity of a network does not necessarily represent the proficiency of the network in an evacuation situation. Although transportation network has hundreds of thousand links, and the impact of their failure to the evacuation varies. Identifying which link is critical to the evacuation performance is challenging but meaningful. Existing studies mostly select the critical links based on the travel performance measurement, such as travel time, travel delay, capacity etc. While during an evacuation, life safety is of the most concern. Therefore, in this research, the critical link is determined by studying the mortality rate before and after the link failure.

3. METHODOLOGY

3.1. Agent-based Modeling Platform

The agent-based modeling and simulation framework is coded in NetLogo to evaluate the near-field tsunami evacuation under transportation network disruptions. Netlogo is a high level integrated modeling platform through agent-based programming language (Wilensky, 1999). This modeling framework enables the multi-parameter exploration for an emergent phenomenon in a multi-agent system and visualizes the dynamic (time-dependent) scenarios. This feature has turned NetLogo into an increasingly popular tool for research due to its extensive documentation, user-friendly interface, expandable modeling environment, the existence of good tutorials, and a large library of preexisting models (Wilensky, 1999; Klugl and Bazzan, 2012). The major part of complexity in evacuation modeling is largely driven by interactions between agents that capture the emergent behavior of the whole system. Along with these benefits, the GIS compatibility in NetLogo further validates the use of this platform for modeling and simulating the evacuation dynamics at a community scale, ranging from engineering studies to sociology. Figure 3.1 shows a snapshot of the simulation environment coded in NetLogo. As shown in Figure 3.1, blue shade shows the tsunami wave, and darker blue represents higher waves. Red dots represent the evacuees who were caught by the tsunami inundation, and the orange dots represent the evacuees who are on the way towards the shelters. Yellow circles represent the locations of primary evacuation shelters, and green represents the evacuees who are safely evacuated to one of the safe areas.

It is noteworthy that the simulation we developed only focuses on the consequences of the tsunami hazard, and we do not include direct consequences of the earthquake on the population or the constructed environment. This is a reasonable assumption since

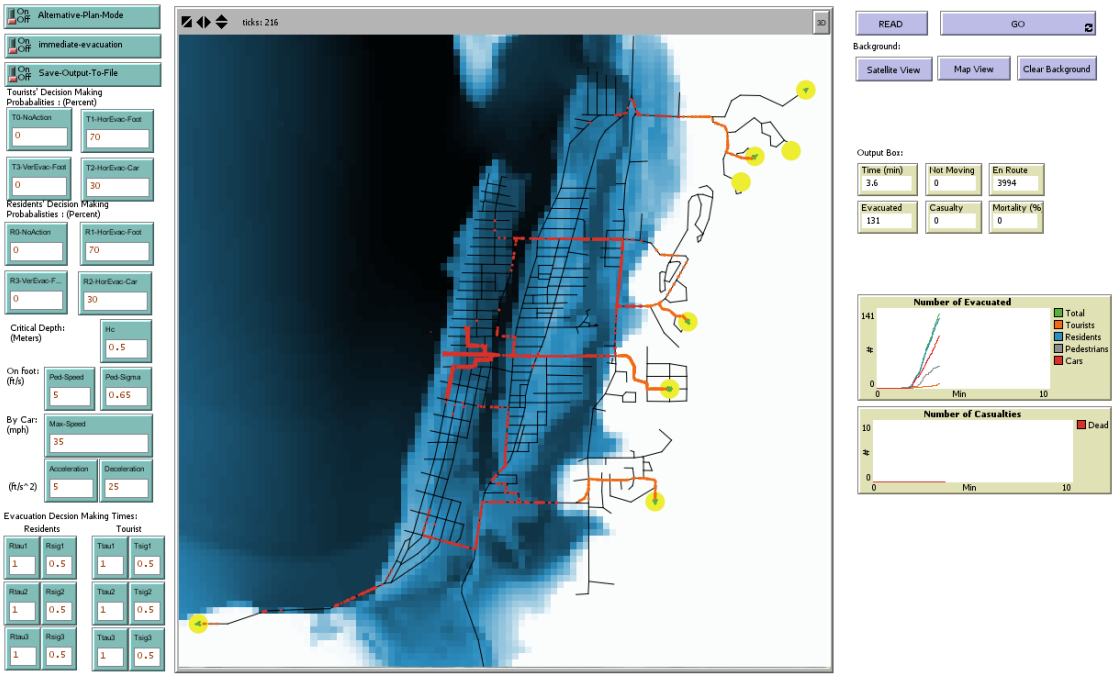

FIGURE 3.1: The NetLogo tsunami model of Seaside, Oregon

over 90% of the loss of life in the 2011 Tohoku disaster was attributed to the tsunami inundation and not the preceding earthquake. The ABM platform, however, will allow the extension to a multi-hazard model in future work. For the agent behavior, it is assumed that all agents are autonomous and heterogeneous, that their choices are directly influenced by their surrounding environment and also through interactions. To simplify the problem, it is assumed that agents do not change their mode choice decisions throughout the evacuation, that is to say, an agent who starts evacuating by car will not switch to evacuation on foot, and vice versa. For the sake of network disruption assessment, it is assumed all agents decide to evacuate, although previous experiences have shown that a small portion of people chose to stay (Mas et al., 2011, 2012; Mas and Koshimura., 2012; Mas and Koshimura, 2012).

3.2. Study Area

For this study, the near-field tsunami arising from the Cascadia Subduction Zone (CSZ) is modeled as shown in Figure 3.2(a). The CSZ measures 1000 km in length and extends from the Mendocino Ridge off the coast of northern California to northern Vancouver Island, British Columbia (Figure 3.2(a)). A near-field event generated from the CSZ is expected to cause widespread damage to the northwest Pacific coast of North America with the first waves arriving in the tens of minutes. The last great CSZ event occurred more than three centuries ago on 26 January 1700 and was a full-length rupture. The event is estimated to have had a moment magnitude (M_W) between 8.7 and 9.2, and a slip of 19 m (Satake et al., 2003). The average recurrence interval between full-length CSZ events is 530 years, and the next event is estimated to have a 7-12% probability of occurrence by 2060 (Goldfinger et al., 2012).

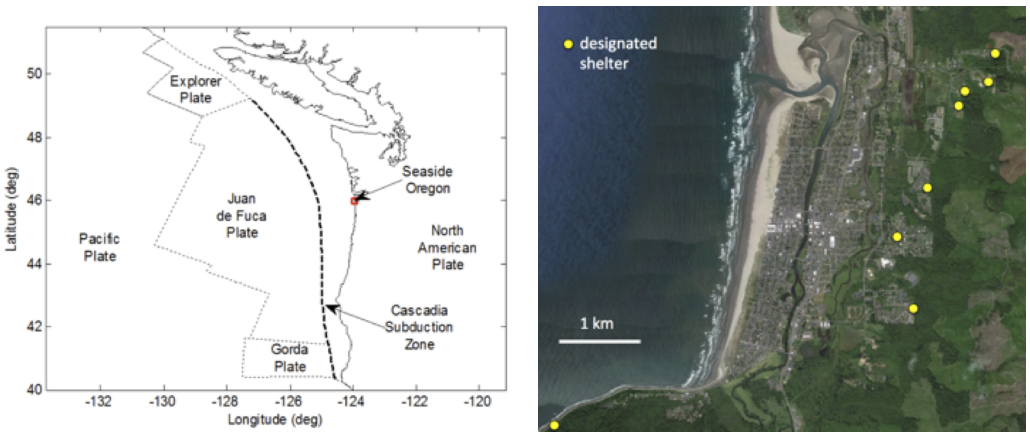

(a) (b)

FIGURE 3.2: (a) Location of cascadia subduction zone; (b) Overview of Seaside, OR (Wang et al., 2015)

The city of Seaside (Figure 3.2(b)) has recently been the topic of several studies regarding tsunami evacuation as well as seismic resiliency and vulnerability, mainly

due to its location and its topography which makes it highly prone to experience CSZ tsunami (Wood, 2007). This is due, in part, to the proximity to the CSZ (Figure 3.2(a)), fairly flat topography, and the location of the tsunami shelter areas at more than 1.5 km from the shoreline. Two rivers, flowing from south to north, divide the city into three parts. The presence of ten bridges in total, spanning these two rivers, makes multi-modal evacuation more complex and highly vulnerable, and makes Seaside an interesting case study for further analysis on the effects of a network disruption on the success rate of tsunami evacuation and mortality rates. The current tsunami evacuation plan for the area calls for horizontal evacuation on foot, and the option of vertical evacuation has only been discussed in recent years as a possible option. No comprehensive studies exist which explore the feasibility of vertical evacuation. In addition to Seaside, there are several other towns along the coast with a high risk of near-field tsunamis, including Ocean Shores, WA, and Long Beach, WA (Wood and Schmidtlein, 2013).

3.3. Model Behavior Overview

Figure 3.3 shows an example of the model simulation starting with time $t = 0$ representing the end of the initial shaking due to the earthquake to the end of evacuation scenario. For this simulation, it is assumed that no evacuation takes place during the earthquake itself. Figure 3.3(a) shows the initial population, shown with brown color, which are distributed normally around the centroid of the beach and downtown area. The agents have the options to evacuate either on foot or by car. Agents change color and shape depending on their mode of transportation (Figure 3.3(b,c). Blue color represents the cars and orange represents the pedestrians. Figure 3.3(b) shows $t = 10$ after the end of earthquake that most of the evacuees have started their evacuation. However, there are many agents who have delayed and they are still in the beach area. Looking at

Figure 3.3(c,d), after approximately 30-35 minutes, the first waves of tsunami reach the shore. Figure 3.3(e) shows the first fatalities that occur when the inundation level exceed 0.5 m, represented as agents with red color. It can also be seen that the tsunami has inundated the first part of Seaside after 40 min, crossing the Necanicum River. Finally, the tsunami reaches the runup limit approximately 1 km inland, 15 minutes after reaching the shoreline (Figure 3.3(f)). At the end of each simulation, the mortality rate of the evacuees can be calculated and be used as a measurement of effectiveness.

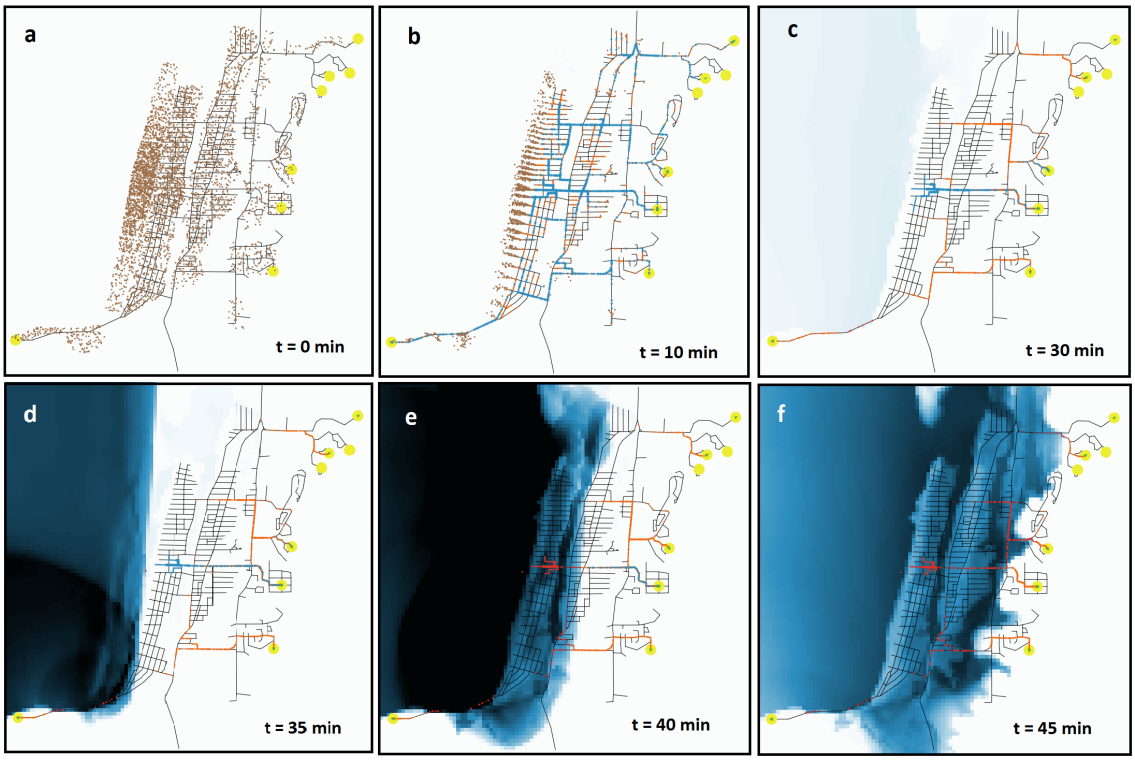

FIGURE 3.3: Example of model simulation

3.4. Monte-Carlo Simulation

To capture the stochasticity of the simulations, mostly due to the distribution of evacuees with different decision-making parameters and walking speeds, Monte-Carlo sim-

ulation has been implemented in Netlogo and R, bridging the gap using package "RNetLogo"[1] in R. RNetLogo is an open-source package that delivers either a headless interface or a GUI to use Netlogo in R. It provides the functions to run models, execute commands, and push or get values from Netlogo directly in R. It allows the modeler to virtually and systematically control NetLogo using R code. The package has been thoroughly documented, providing the opportunity to run simulations, store the results, and analyze using powerful statistical tools in R (Thiele, 2014). Therefore, the assessments have been done using a Monte-Carlo simulation mostly with 10 times repetition.

3.5. Model Components

There are essentially five building blocks of the model: population distribution, road network, tsunami inundation data, the locations of evacuation shelters, and casualty model, each of which is explained in detail below.

3.5.1 Population Distribution Model

There can be a high spatial-temporal variability of community population distribution based on factors such as the weather, time of day, week, or season (Wang et al., 2015). Moreover, a given population will contain a number of different segments such as residents or visitors who will respond differently for a given hazard (Wang et al., 2015). It is also of great significance to pinpoint whether evacuation planning is being considered for a specific time frame. For instance, night time in winter where almost all residents are located at their residence and the city is almost empty of tourists is completely different from a noon time on the weekend in the summer when most residents are packed at the beach and downtown area, and the population of the city is, in extreme cases, doubled by the number of tourists.

[1] `https://cran.r-project.org/web/packages/RNetLogo/index.html`

In the model, the worst case scenario, known as noon-time of a weekend in the summer, is being considered. Tourists and residents are distributed unevenly based on the attributes of the environment (i.e., tourist attractions and residential areas) to the 38 areas shown in Figure 3.4. These areas are chosen such that the change in land use and other attributes is minimal in each region. As shown in Figure 3.5, the population is normally distributed around the centroid of the beach and the downtown area. Therefore, the concentration of the evacuees in those two areas is high. Moreover, although different categories of people (i.e., residents and tourists) may respond differently to the same hazard and categorization of the evacuees based on their attributes should be considered for a realistic evacuation simulation platform, for the sake of the main objective of this study it is assumed that different categories react to the hazard in the same fashion. Meaning that they choose their destination, their route, their mode of transportation, and immediacy of evacuation regardless of their knowledge and familiarity with the area.

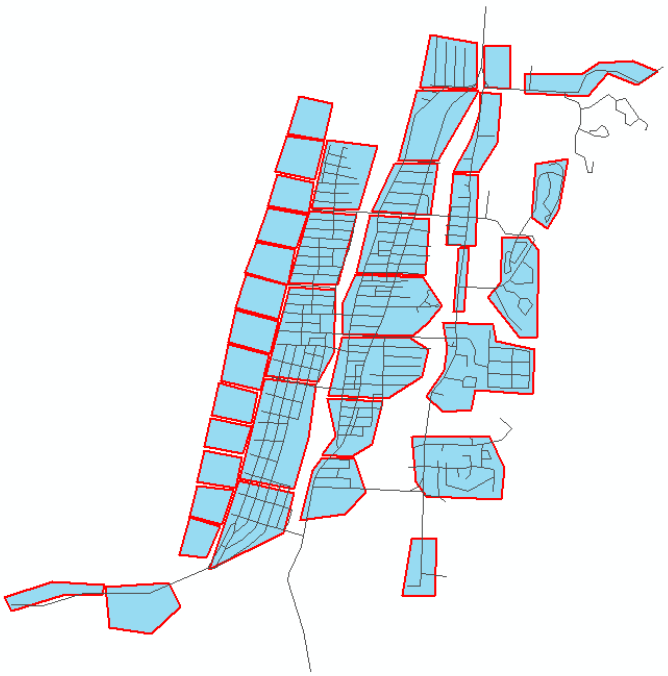

FIGURE 3.4: Boundaries of regions, Seaside, OR

According to US Census data, the latest population of the city of Seaside is estimated to be 6445 with 20% under the age of 18 [2]. The number of tourists in the city, considering the amount of rentals, hotels, and inns can be up to 10,000. However, due to computational challenges in Netlogo coming from agent-agent interactions, 4500 evacuees have been included in the simulation runs. Although this assumption is not realistic, however, for the purpose of network assessment and also relative comparison regarding the sensitivity of the mortality rate to the influential factors, it stays valid.

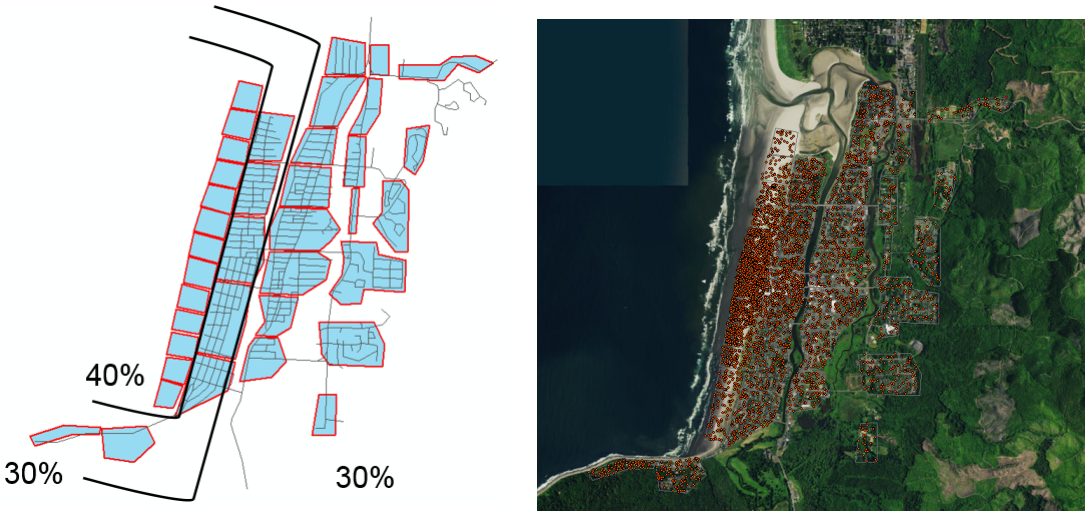

(a) (b)

FIGURE 3.5: Population distribution

3.5.2 Road Network

The road network is imported into the model as a GIS shapefile which was extracted from OpenStreetMap [3] with markings for the area of interest. It is assumed that all the agents (i.e., residents and visitors) are to follow this network, including the potential crossing of 10 two-lane bridges. For the purpose of network assessment, the possibility of

[2] http://www.cityofseaside.us/

[3] http://www.openstreetmap.org

network disruption in the form of link accessibility, limiting access to (a) neither pedestrians nor cars and (b) pedestrians only is considered. In the simulation, it is assumed that all the agents (i.e., residents and tourists) have to follow the road network to the tsunami shelters. The use of other alternatives such as swimming across the river or cutting through fields or parking lots are prohibited in this model. In other words, pedestrian shortcuts are not considered in the model. Conservatively, all network links are considered as one-way one-lane streets with a speed limit of 35 MPH. This is a reasonable assumption based on the speed limits (maximum allowable speed) of the area and field observations of the general standing of the network. In the beginning of the simulation, all the agents head to the nearest link, and later on, based on the decision-making probabilities which will be explained later, they choose either to evacuate on foot or by vehicle.

3.5.3 Tsunami Shelters

Oregon Department of Geology and Mineral Industries has proposed eight evacuation shelters outside the inundation zone as shown in Figure 3.6 (Priest et al., 2013). These are the primary evacuation locations in the model. However, Wang et al. (2015) have studied the effect of the vertical evacuation shelters. For the sake of the main objectives of this study, the focus is on the primary evacuation shelters. All shelters are assumed to have the capacity to fit the evacuees. In addition, it is assumed that all shelters are structurally sound and can withstand tsunami and earthquake forces (FEMA, 2008).

3.5.4 Tsunami Inundation

The inundation modeling comes from the ComMIT/MOST model developed by NOAA calibrated for Cascadia Subduction Zone (Titov and Gonzalez, 1997). Inundation is modeled as an extreme event with a 2500-year return interval (Venturato et al., 2007). The inundation model supplies time variation of flow depth and speed for the area of interest. The speed of the flow, for simplification purposes, and due to the fact that there is still

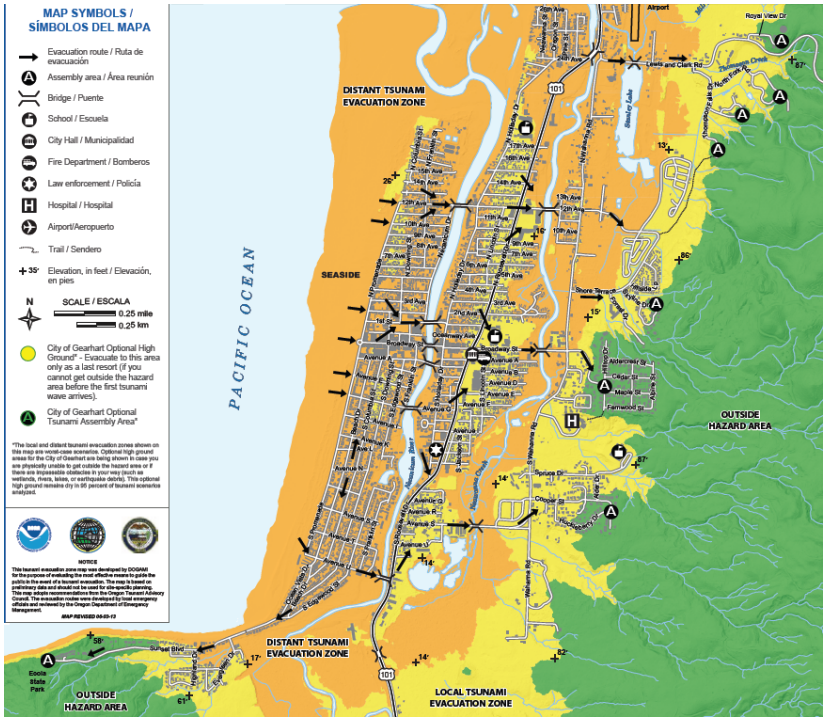

FIGURE 3.6: Evacuation shelters of Seaside, OR (FEMA, 2008)

no comprehensive casualty model incorporating flow speed, has been neglected, and only flow depth is imported into the model. Although these models use a "bare earth model" and do not consider the impact of natural vegetation, man-made structures, or roughness of the surface on the inundation strength, the assumption will still be conservatively valid. However in a few cases, the constructed environment could cause an increase in flow speed along links which are parallel to the main flow direction (Park et al., 2013).

3.5.5 Casualty Model

Although calculating the rate of casualties can be highly complicated due to the variability of a person's age, gender, mental and physical state (Yeh, 2010), the casualty model in the simulations is simplified. Basically, if a wave with a height of H_c or more touches an agent, it will be considered as the casualty. This assumption might not reflect an accurate mortality rate; however, for comparison purposes and assessment of the trans-

portation network, this gives us a reasonable estimate of mortality rate. Besides, H_c can reflect the vulnerability of the evacuee community to the inundation force. For example, in a population with high percentages of elderly and children the vulnerability is high, and therefore, the H_c can be adjusted to lower values. The H_c for these simulations has conservatively been set to be 0.5 meters. Model casualties beyond the initial (approximately 1 hr) inundation such as hypothermia or heart attack are not modeled.

3.6. Agent Decisions

For a given population, road network, tsunami shelter, and inundation scenario, the model can be ran with several options related to human decisions and are described below.

3.6.1 Mode Choices

It is assumed that the agent is located at ground level and outside. In other words, it is assumed they are not in their car, nor are they in a building that would provide them shelter if no actions were taken. Each agent can make one of the following choices. Option 1 is horizontal evacuation on foot. For this option, it is assumed that the agent is knowledgeable of the most efficient route to the nearest tsunami shelter outside the inundation zone. Option 2 is horizontal evacuation by car. Similar to Option 1, it is assumed that the agent knows the most efficient route. It is also assumed that the car is located nearby and the time that it takes to go to the car is modeled and accounted for in the milling time as discussed in the next section.

The probability of choosing an option can be specified by the evacuee population. For example, for a given simulation, the population may have 70% who choose horizontal evacuation on foot (Opt. 1) and 30% who choose horizontal evacuation by car (Opt. 2). As mentioned earlier, it is assumed that agents act independently of others, meaning that there are no social group influences.

3.6.2 Milling Time

One of the most challenging aspects of modeling natural hazard evacuation, especially for near-field tsunami evacuations with very low preparation time, is to model evacuation milling time. Milling time depends on the quality and reliability of the messages conveyed regarding the evacuation, performance of the decision makers, and public response to the messages (NRC, 2006). Although many researchers focus on the evacuation preparation time of natural hazards with long preparation times (Lindell and Prater, 2007; Kang and Prater., 2004), rapid-onset hazards such as tsunamis still need to be examined thoroughly (NRC, 2006). It has been shown that milling time has a great impact on both the formation and evolution of bottlenecks and traffic congestions (Naser and Birst, 2010), and mortality rates of scenarios (Wang et al., 2015). To capture the evacuation preparation time, as suggested by Mas et al. (2011), departure times follow a Rayleigh distribution as shown in figure 3.7.

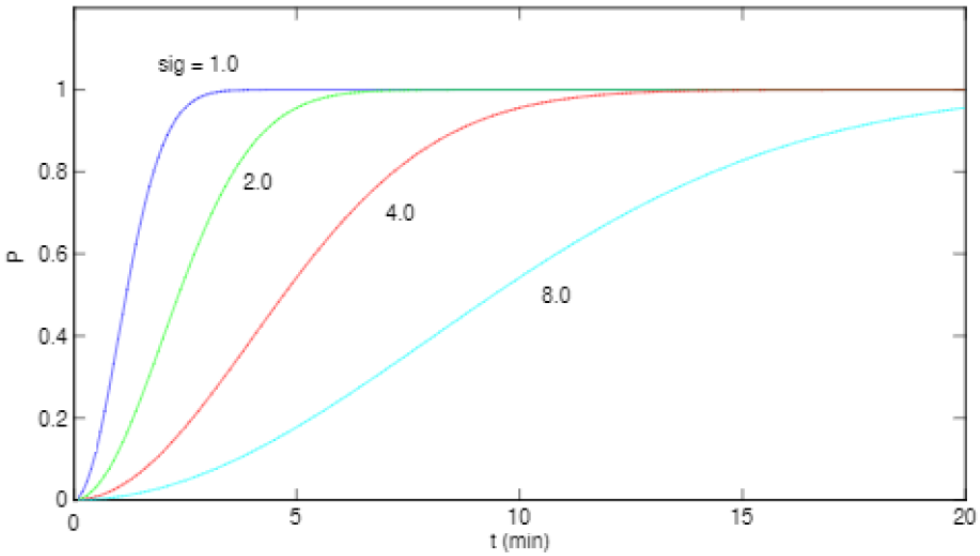

FIGURE 3.7: Representation of milling time with σ and τ using Rayleigh distribution (τ = 0) (Wang et al., 2015)

Understanding psychological aspects involved in the process of departure time decision-

making is complex. It depends on the perceived immediacy of the threat as well as the required action (Sorensen, 2000). To abstractly consider the decision-making process, values of τ and σ are reasonably calibrated and the milling time is randomly drawn from the mentioned distribution with the following formula (Tweedie et al., 1986; Lindell and Prater, 2007).

$$P(t) = \begin{cases} 0 & 0 < t < \tau \\ 1 - e^{-(t-\tau)^2/(2\sigma^2)} & t > \tau \end{cases} \tag{3.1}$$

Where t is the departure time in minutes after earthquake. Both τ and σ can be adjusted in the platform. τ represents the minimum time that an evacuee needs to get prepared, and σ represents the spread of the departure times. The larger the σ is, the larger the tail of the distribution towards later departure times will be. Slight increases in τ and σ will lead to an enormous increase in mortality rates (Wang et al., 2015). For the sake of the main objective and having accurate analysis on the vulnerability of transportation network, and following the suggestion of government officials regarding the importance of immediate evacuation, it is assumed τ to be 1 minute and σ to be 0.5, meaning that 99 percent of agents start their evacuation between 1 to 2 minutes and 30 seconds. 3.1 represents the percentage of different departure time for different values of σ.

TABLE 3.1: Time in minutes required for agents to initiate an action as a function of σ ($\tau = 0$) (Wang et al., 2015)

σ	Percentage of agents initiating actions		
	50%	95%	99%
1.0	1.2	2.4	3.0
2.0	2.4	4.9	6.1
4.0	4.7	9.8	12.1
8.0	9.4	19.6	24.3

3.7. Vehicular Movement

The movement of vehicles is governed by the classic car-following model, General Motors model, with the following equation.

$$a_{n+1}^{t+\delta t} = [\frac{\alpha_{l,m}(v_{n+1}^t)^m}{(x_n^t - x_{n+1}^t)^l}](v_n^t - v_{n+1}^t) \tag{3.2}$$

where:

x_n^t = Location of leading vehicle at time t

v_n^t = Speed of leading vehicle at time t

x_{n+1}^t = Location of following vehicle at time t

v_{n+1}^t = Speed of following vehicle at time t

v_{n+1}^t = Speed of following vehicle at time t

l = Distance headway exponent (Varying from -1 to +4)

m = Speed exponent (Varying from -2 to +2)

$\alpha_{l,m}$ = Sensitivity coefficient

δt = Perception-Reaction time

The parameters are adjustable and can be calibrated using empirical data. However, due to lack of empirical data regarding the driving behavior in emergency situations, the following parameters set has been chosen to simulate the vehicular movement. The perception-reaction time is known to be lower than usual in emergency situations since the drivers tend to be more alert and responsive if they are aware of the approaching threat. Therefore, the perception-reaction time in this case, conservatively and in favor of evacuation by car, is assumed to be fairly close to zero.

It is worth mentioning that the combination of parameters above, with the assumption of steady state traffic flow, from a macroscopic point of view, leads to well-known Greenshield model (citation) which represents a linear relationship between speed and density. Below is the derivation of parameter α.

TABLE 3.2: Car-following model parameters

Parameter	Notation	Value
Distance Headway Exp.	l	2
Speed Exp.	m	0
Perception-Reaction Time	δt	0
Sensitivity Coef.	α	0.14

$$a_{n+1}^{t+\delta t} = [\frac{\alpha_{l,m}(v_{n+1}^t)^m}{(x_n^t - x_{n+1}^t)^l}](v_n^t - v_{n+1}^t) \tag{3.3}$$

$$a_{n+1}^{t+0} = [\frac{\alpha_{2,0}(v_{n+1}^t)^0}{(x_n^t - x_{n+1}^t)^2}](v_n^t - v_{n+1}^t) \tag{3.4}$$

$$a_{n+1}^{t} = [\frac{\alpha_{2,0}}{(x_n^t - x_{n+1}^t)^2}](v_n^t - v_{n+1}^t) \tag{3.5}$$

$$\ddot{x}_{n+1}^{t} = [\frac{\alpha_{2,0}}{(x_n^t - x_{n+1}^t)^2}](\dot{x}_n^t - \dot{x}_{n+1}^t) \tag{3.6}$$

Let $h = x_n^t - x_{n+1}^t$, then we have:

$$\ddot{x}_{n+1}^{t} = \frac{\alpha_{2,0}}{h^2}\frac{dh}{dt} \tag{3.7}$$

$$\frac{dv}{dt} = \frac{\alpha_{2,0}}{h^2}\frac{dh}{dt} \tag{3.8}$$

$$dv = \frac{\alpha_{2,0}}{h^2}dh \tag{3.9}$$

$$\int dv = \int \frac{\alpha_{2,0}}{h^2}dh \tag{3.10}$$

$$v = \frac{-\alpha_{2,0}}{h} + c \tag{3.11}$$

Plugging in the boundary conditions for Jammed state and free flow state, we have:

$$\alpha K_j = c \tag{3.12}$$

$$c = V_f \tag{3.13}$$

$$\alpha = \frac{V_f}{K_j} \tag{3.14}$$

if we assume free-flow speed, V_f, equals 35 mph and jam density, K_j, equals 250 vpm, α is estimated as following.

$$\alpha = 0.14 \frac{mi^2}{hr} \tag{3.15}$$

In addition, parameter α linearly correlates with the range of accelerations and decelerations calculated from the car-following model. Therefore, it has to vary in a reasonable and realistic manner. Simulations have shown that α of 0.14 leads to accelerations in the range of 5 ft/sec^2 to 10 ft/sec^2. Decelerations on the other hand vary from 10 ft/sec^2 to 25 ft/sec^2. Based on the literature, this range of accelerations and decelerations represent the empirical data fairly well, considering the fact that in the case of evacuations accelerations and decelerations tend to be higher. Therefore, changes in α are not suggested. However, the sensitivity of this parameter on the evacuation efficiency is deeply investigated in the next chapter.

Car-following model coded in the model should ideally result in a Greenshield relationship between variable speed and density. Figure 3.8 shows the Speed-Density diagram generated by the evacuation simulation model. This further validates the expected behavior of the model. As shown in figure 3.8, speed decreases with when density increases. In

addition, the graph is highly concentrated around higher densities which shows that the network is in a congested phase.

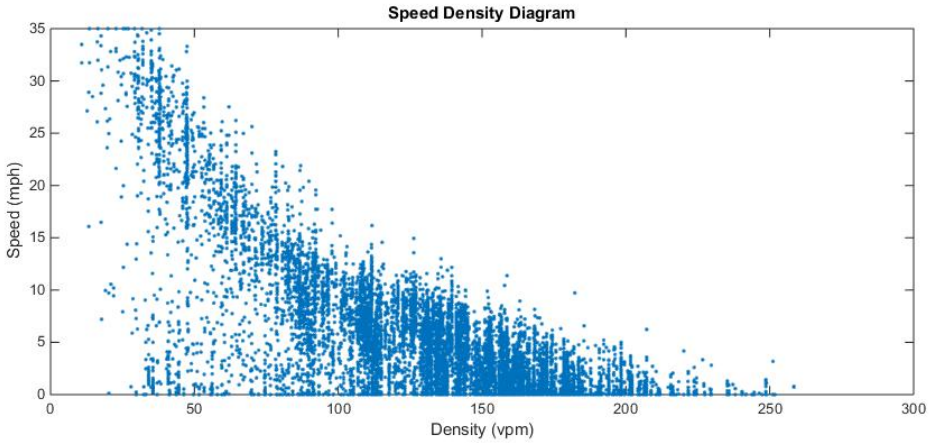

FIGURE 3.8: Speed density diagram

3.8. Pedestrian Movement

The speed of evacuation is another significant variable governing hazards evacuation (Wood and Schmidtlein, 2012). Normal walking speed is on average 4.5 ft/s (1.37 m/s). For the simulation of near-field tsunami evacuation, although people tend to walk faster in emergency situations, the mean walking speed is conservatively set to be 4 ft/s (Knoblauch et al., 1995). To capture the walking speeds of the elderly, children, and also, fast walkers, it is assumed that walking speeds follow a normal distribution. Conservatively, the normal distribution's standard deviation is set to 0.65 ft/s (0.2 m/s) which, as is shown in figure 3.9, covers very slow walking to slow running, ranging from 1.5 to 5.5 ft/s (TRB, 2010). The effect of tiredness of evacuees and topography of the environment have been neglected in this simulation. Each pedestrian agent is assigned a walking speed which will not vary over the simulation. All evacuees begin to evacuate by foot to the nearest road. From there, agents with different decisions are separated. The

time required to access their cars for agents who choose not to evacuate by foot is assumed to be modeled by their milling time.

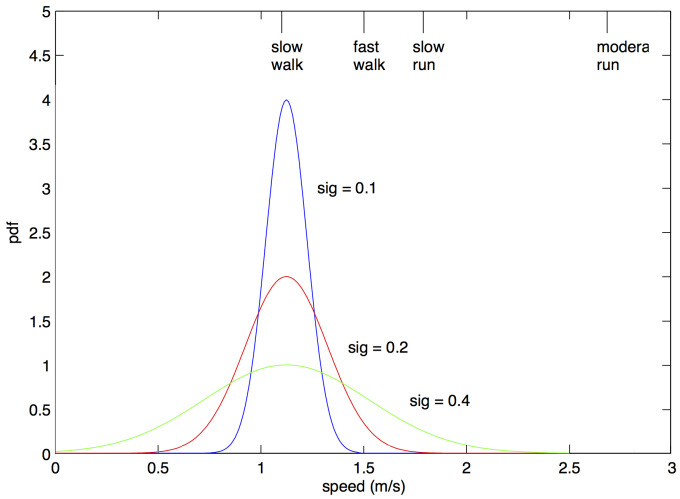

FIGURE 3.9: Walking speed distributions (Wang et al., 2015).

3.9. Summary

In this section, the development of the agent-based multi-modal tsunami evacuation platform is elaborated, along with its components and procedures. In summary, the coded platform consists of five different components, the population distribution model, the transportation network, evacuation shelters, the tsunami inundation, and the casualty model. The simulations are bound with evacuees' characteristics which are translated to the evacuees' decisions, such as choice of evacuation mode, start-time of evacuation (milling time), and walking speed which represents the physical ability of the evacuee. In addition, vehicular movement and the vehicle-to-vehicle interaction following the General-Motors car-following model has been described in this section. In the next section, the modeling results of the general evacuation behavior, the factors involved, and their impact on the mortality rate of the scenario and evacuation efficiency is presented.

4. RESULTS: MULTI-MODAL EVACUATION BEHAVIOR

Understanding of evacuation behavior is critical for emergency responders to develop an optimal evacuation plan, and loss of life can therefore be minimized. In this chapter, the behavior of the evacuation under the influence of different control parameters is assessed. Further, recognizing the travel pattern in evacuation is beneficial for traffic control. Evacuation trajectory is therefore extracted from the simulation and displayed in 3-D graph for travel pattern analysis.

4.1. Model Behavior

Various factors can affect evacuation performance such as mode choices, the minimum milling time, the walking speed, the maximum driving speed, the car-following behavior, and critical tsunami inundation depth. Hereunder, the sensitivity analysis of the mortality rate of the evacuation against the factors affecting the efficiency of the scenario is presented.

4.1.1 Evacuation Mode

The mode choice of the agents based on their decision-making attributes can be implemented in the model by defining the percentage of agents choosing any particular evacuation mode. Studies have shown that the evacuees' mode choice decision has significant impacts on the mortality rate (Wang et al., 2015). To test the capability of the model to simulate traffic congestion besides the evacuation on foot, agents choosing horizontal evacuation by either foot (Option 1) or by car (Option 2), varying the percentage from 0 (all with the car) to 100% (all on foot) are considered. As shown in Figure 4.1, if it is assumed that the percentage of the agents who decide not to evacuate is minimal or

close to zero, the increase in the percentage of pedestrians will lead to much lower mortality rates. Use of cars is not recommended by officials for evacuation purposes since this will lead to creating bottlenecks and heavy congestion which will cause very higher travel times (Spiess, 1990).

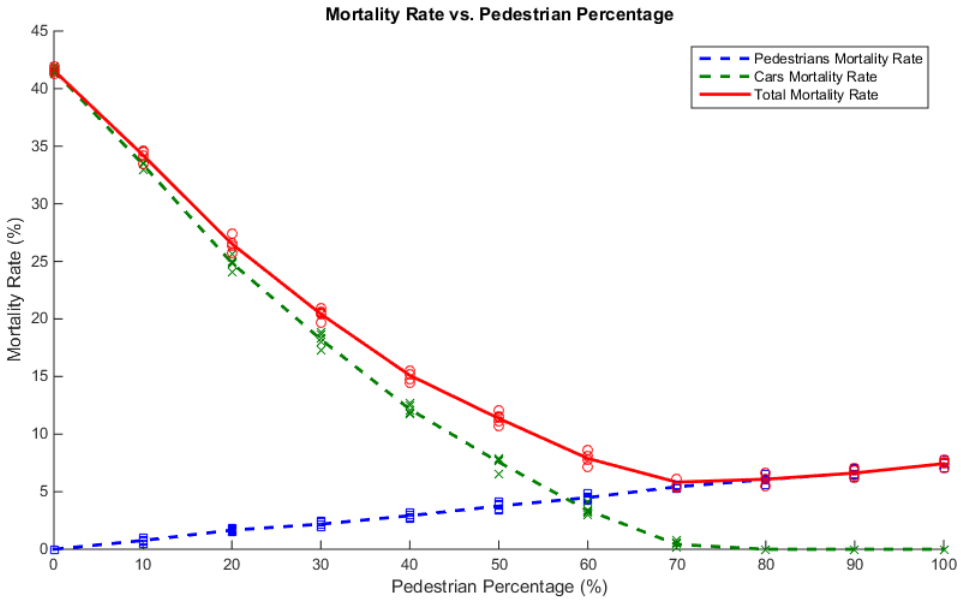

FIGURE 4.1: Impact of percentage of pedestrians on mortality rate

To capture the stochasticity due to evacuation walking speeds and the spatial variation of decision making, the mortality rates are the average of 10 simulation runs. As shown in figure 4.1, for the percentage of pedestrian higher than 70, the total mortality rate changes slightly above the minimum value, shown in red. The green curve shows the contribution of cars in total mortality rate. As shown in figure 4.1, the mortality rate of the cars decreases exponentially as the percentage of the pedestrians increases, since traffic congestion conditions will likely increase as the number of vehicles on the road increases at any time, especially on several roads that lead to the evacuation shelters (Spiess, 1990). For example, the contribution on cars to the mortality rate increases by a factor of 5.5 if the percentage of evacuees who drive increases from 50% to 100%. On the other hand, the

mortality rate of pedestrians linearly increases, shown in the blue curve, with an increase of evacuees who decide to evacuate on foot. Again, the trade off between mortality of cars and pedestrians reaches it's maximum when the percentage of pedestrians goes to 70%.

In this scenario, several assumptions that minimized congestion and increased the survivability of agents traveling by car, including unlimited car capacity at each tsunami shelter and basic interaction of cars and pedestrians were made. Furthermore, probability of accidents or breakdowns that would increase delays was not included, nor were the number of agents who would abandon their cars and continue on foot modeled. Factors like technological failures (i.e., signal lights) that would affect surface transportation were not included. Future efforts will have to consider these factors to develop more realistic scenarios for multi-modal tsunami evacuation.

4.1.2 Minimum Milling Time

As discussed in Section 3.6.2, the decision time with two parameters τ and σ, where τ represents the delay time (no agents evacuate for $t < \tau$) and σ is a scale parameter representing the variability in the cumulative probability distribution based on a Rayleigh distribution were modeled. Although in reality, both τ and σ can be varied based on an agent's classification (e.g., resident or transient) and evacuation choice, only the impact of τ on efficiency of the evacuation scenario were assessed, since both of the parameters are expected to have somewhat similar impact on the mortality rates.

Figure 4.2 shows the model sensitivity to τ. For this scenario, σ is kept constant ($\sigma = 0.5$) and τ varies from 0 (immediate evacuation) to 20 minutes. As expected, the mortality rate increases significantly as the delay time increases, regardless of the walking speed of the scenario. Moreover, the effect of minimum milling time gets more significant as the number of evacuees on foot increases. Likewise, comparing Figures 4.2(a) and 4.2(b), for scenarios with lower walking speeds, the impact of minimum milling time on mortality rate is higher as well.

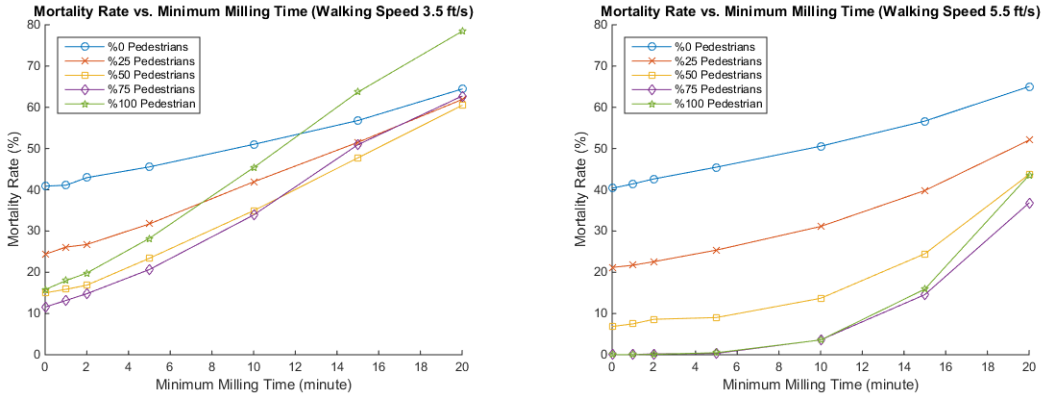

(a) Walking Speed = 3.5 ft/s (b) Walking Speed = 5.5 ft/s

FIGURE 4.2: Impact of minimum milling time on mortality rate

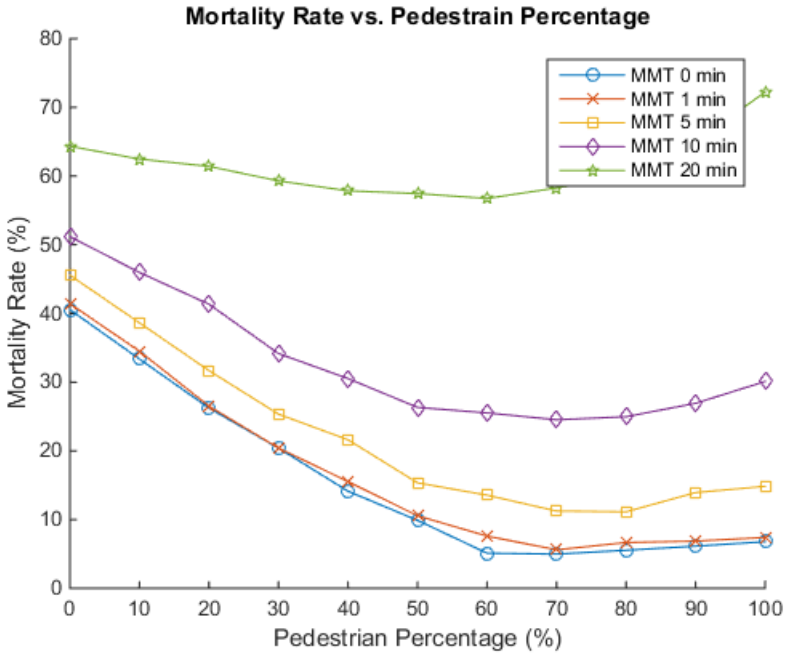

FIGURE 4.3: Impact of minimum milling time on optimal evacuation mode split

The impact of minimum milling time on the optimal split of evacuation mode is further investigated. Figure 4.3 shows the variation of mortality rate due to changes in the percentage of pedestrians for different minimum milling times. In General, the impact of milling time is significantly greater on pedestrians than on the cars. Comparing two extreme cases where all the evacuees evacuate by car and all the evacuees evacuate on foot, it can be concluded that mortality rate increases from 40% to 65% and from 10% to 70% respectively if minimum milling time goes from 0 to 20 minutes. This phenomenon causes the optimal evacuation mode split to vary according to different minimum milling times. In addition, there is a critical threshold for minimum milling time, beyond which fully evacuation by cars results in lower mortality rates, expectedly around 15 minutes.

4.1.3 Walking Speed

Figure 4.4 shows the effect of the walking speed on mortality rate where the walking speed is modeled as a normal distribution with mean speed (u) and standard deviation sigma (σ). For these simulations, two different minimum milling times, $\tau = 1$ and $\tau = 15$ minute delay from the time of the earthquake to the start of evacuation with a $\sigma = 0.5$ were used (i.e., 95% of the population would have taken action approximately 5 or 20 minutes after the earthquake in either case respectively).

As expected, Figure 4.4 shows that the walking speed has a strong influence on the mortality rate. As expected, the influence of average walking speed increases as the percentage of pedestrians increase in both proposed milling time cases. In addition, the comparison between figure 4.4(a) and 4.4(b) shows that walking speed is significant for higher milling times. For example, focusing on evacuation scenario with 100% pedestrian, an increase in walking speed from 3.5 to 5.5 ft/s decreases the mortality rate by 45% in the case of 15 minutes minimum milling time. On the other hand, the decrease can be less than 20% if the milling time is as low as 1 minute.

Moreover, for low minimum milling times, the average walking speed of 5 ft/s and

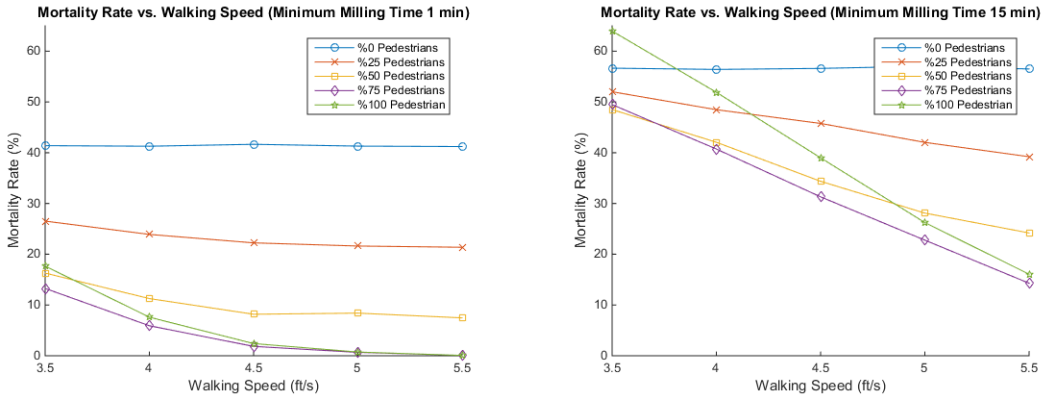

(a) Minimum milling time = 1 minute (b) Minimum milling time = 15 minutes

FIGURE 4.4: Impact of walking speed on mortality rate

higher would have all the same impact on the efficiency of evacuation. On the other hand, for higher milling times, mortality rate keeps linearly decreasing with increase in average walking speed.

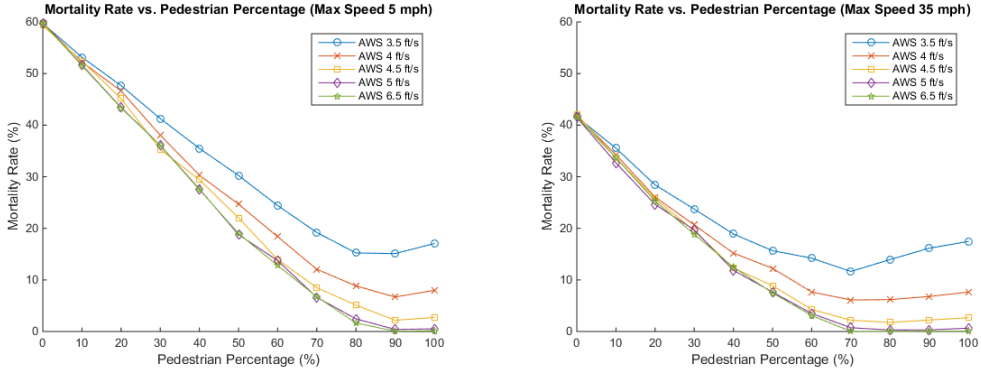

(a) Maximum driving speed = 5 mph (b) Maximum driving speed = 35 mph

FIGURE 4.5: Impact of walking speed on the optimal evacuation mode split

It is also of great value to assess the impact of walking speed on the evacuation efficiency, along with the maximum driving speed of the cars which indirectly reflects the advantage of cars to pedestrians. Figure 4.5 shows the impact of walking speed for two evacuation simulation scenarios with two different driving speed limits. Here, minimum

milling time is set to be 1 minute. As expected, increase in average walking speed moves the optimal split of evacuation mode towards pedestrians. Looking at figure 4.5(a), it can be observed that optimal split shifts from 100% pedestrians to 80% pedestrians as average walking speed decreases from 5.5 ft/s to 3.5 ft/s. For the main purposes of this study, although it is expected that the people walk faster in panic situations, walking speed is conservatively considered to be 4 ft/s which represents a moderate walking speed.

4.1.4 Maximum Driving Speed

Maximum driving speed of the cars, speed limit, could be one of the important parameters that not only affects the mortality rate of a specific scenario, but also shifts the optimal evacuation mode choice split towards either higher or lower percentages of pedestrians. Figure 4.6 shows the impact of the driving speed limit on mortality rate for two different evacuation simulation scenarios with the different average walking speed for pedestrians. Both figures 4.6(a) and 4.6(b) confirm that effect of the maximum driving speed for 20 mph and above is negligible, for almost all the evacuation mode splits. This is mainly due to the fact that in a congested network where cars do not get to reach the speed limit, unrealistically high speed limits are not influential to the mobility of the network. However, for maximum driving speed lower than 20 mph, the mortality rate of the scenario increases as the maximum driving speed decreases, and expectedly, the effect goes to zero as the percentage of cars goes to zero. Comparing these two figures, it can also be stated that the impact of an increase in maximum driving speed is slightly greater for the scenarios with a lower average walking speed of pedestrians.

In addition, figure 4.7 shows the impact of maximum driving speed on the optimal evacuation mode split, coupled with different average walking speeds. Looking at Figure 4.7(a), it suggests that the optimal split shifts towards pedestrians as the speed limit decreases to 5 mph and vice versa in the scenarios with lower walking speeds. Similarly, for simulation with higher average walking speeds, the mortality goes to zero earlier with

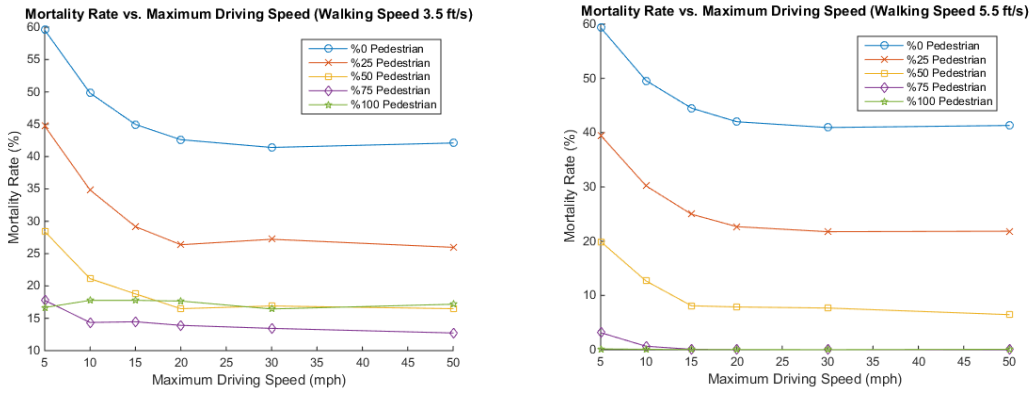

(a) Walking speed = 3.5 ft/s (b) Walking Speed = 5.5 ft/s

FIGURE 4.6: Impact of maximum driving speed on mortality rate

the increase in pedestrian's percentage for cases with the higher maximum driving speed for the cars.

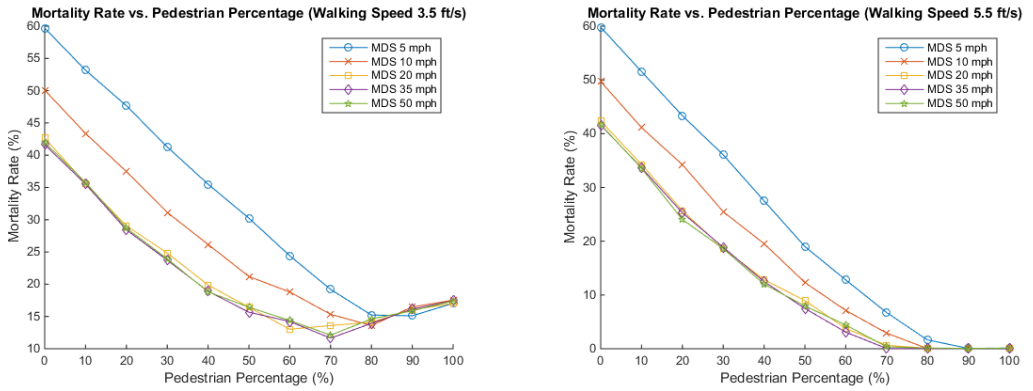

(a) Walking speed = 3.5 ft/s (b) Walking speed = 5.5 ft/s

FIGURE 4.7: Impact of maximum driving speed on the optimal evacuation mode split

4.1.5 Car-Following Model

Another significant parameter that indirectly affects the mortality rate is the sensitivity coefficient in the car-following model, α. As this coefficient directly correlates with the range of acceleration and deceleration of the cars, this variable cannot take a value

higher than 0.14 mi^2/hr since any higher value leads to assumption of jam density higher than 250 veh/mile/lane or free flow speed of higher than 35 mph which is unrealistic. On top of this, any value of α higher than 0.14 results in unrealistic accelerations and decelerations.

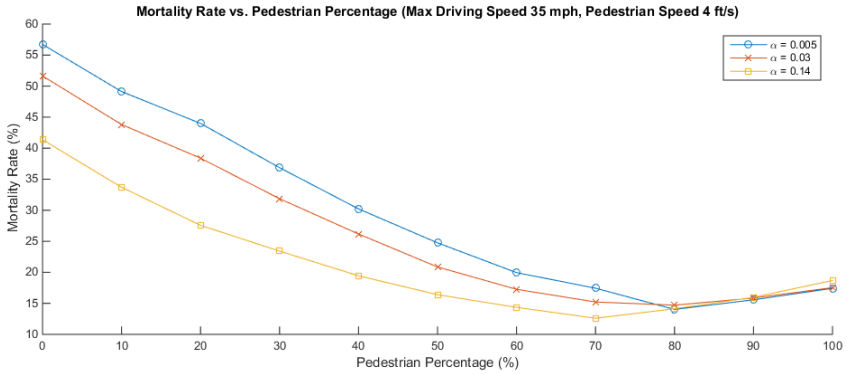

FIGURE 4.8: Impact of car-following model sensitivity parameter

Despite the low variability range of α, Figure 4.8 displays the sensitivity of mortality rate over change in α for the scenario where Maximum driving speed is set to 35 mph, mean walking speed is set to 4 ft/s, minimum milling time is set to 1 minute ($\tau = 1$ and $\sigma = 0.5$). As shown in the figure, lower sensitivity coefficients result in lower accelerations and decelerations, meaning that the cars lose their agility, resulting in higher mortality rates when a significant portion of evacuees are evacuating by car. In addition, with the decrease of parameter α, the optimal evacuation mode split moves towards pedestrians since cars lose their advantage in case of lower accelerations and decelerations.

4.1.6 Critical Depth

Critical depth, the minimum depth of the wave that causes fatality to the agents, can represent the physical vulnerability of the evacuees to the tsunami inundation. For instance, a community with higher number of elderly and children could be more sensitive to the impact force of tsunami inundation, and in that case, the critical depth can be

adjusted to lower values.

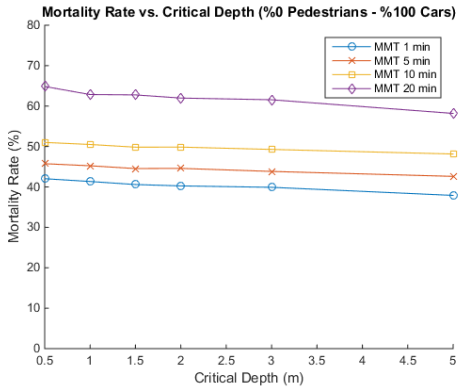

(a) Pedestrian percentage = 0%

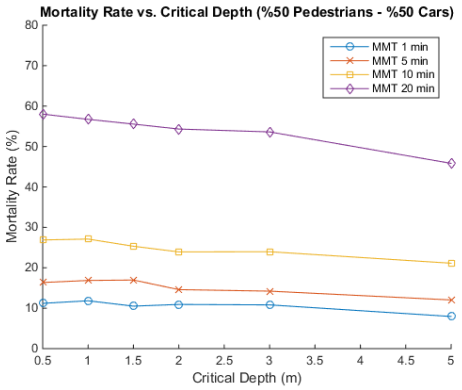

(b) Pedestrian percentage = 50%

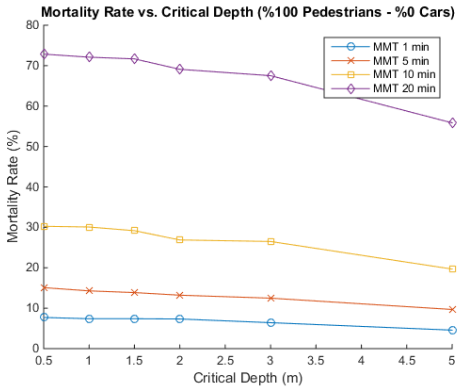

(c) Pedestrian percentage = 100%

FIGURE 4.9: Impact of critical depth on mortality rate

Figure 4.9 shows the mortality rate as a function of critical depth, h_c, used as the criteria to determine the casualty of an agent. For this simulation, which shows the impact of critical depth coupled with mode choice split and minimum milling time, walking speed of 4 ft/s, maximum driving speed of 35 mph, and minimum milling time of 1 minute ($\tau = 1, \sigma = 0.5$) are set. In this scenario, it is shown that generally, mortality rate decreases as the critical depth increases. The impact of critical depth increases with the increase in the percentage of pedestrians. In addition, Minimum milling time

also positively affects the effect of critical depth, meaning that the significance of critical depth increases for higher milling times. This is mainly because of congestion of evacuees in the shoreline due to high milling times when the first waves hit the city. Although the model results were not highly sensitive to the choice of h_c, we can seek improvements to the model by considering alternative casualty models that consider age and gender (Yeh, 2010), hydrodynamic forces (Koshimura et al., 2006), and other factors (Jonkman et al., 2008). However, for further assessment in this study critical depth is conservatively set to 0.5 meters.

4.2. Travel Patterns: Evacuation Trajectory

Evacuation trajectory displays the spatio-temporal characteristics of evacuees. In other words, the position of every single evacuee at any moment can be located from the trajectories. It can also represent the general model behavior and travel patterns. Using trajectories, one can therefore observe the distribution of casualties, the distribution of their starting point, and even the route that they chose. The critical spots can be further recognized and marked. What's more, using the trajectories of safely evacuated agents, safe zones can be identified in the area, and proper evacuation strategies for different parts of the city can be devised. In addition, acquiring empirical data to validate evacuation models are either extremely hard or, in most cases, even impossible. The urgency of near-field tsunami and its rarity in nature, makes it almost impossible to validate this model with empirical data. However, to assess the performance of the model, the evacuation trajectories can be analyzed to ground truth the behavior of the model.

Figure 4.10 shows the trajectories of pedestrians in the case that all the evacuees evacuate on foot. The X axis represents the latitude, the Y axis represents the longitude, and vertical axis represents the time in seconds. Each curve shows the trajectory of

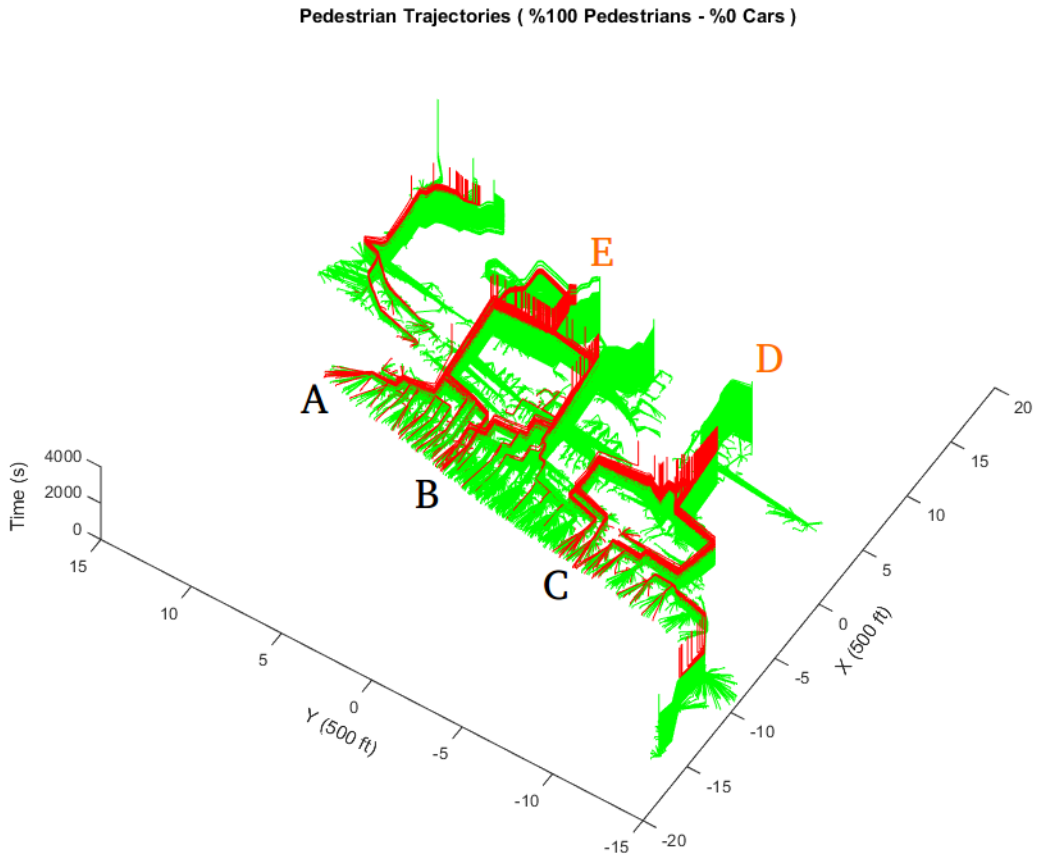

FIGURE 4.10: Pedestrian trajectories - 100% pedestrians

one evacuee, and differentiated by the color. Red curve denotes the trajectory of the casualties, evacuees who were caught by the tsunami inundation, and green reflects the trajectory of the evacuees who safely evacuated into one of the shelters. As exhibited in the casualties'trajectories, their starting location were concentrated in three areas of A, B, and C, and also they headed to one of the shelters (E and D), and they were caught by the tsunami wave somewhere on the road to their destination. Focusing on areas A, B, and C, it is worth mentioning that area B and C are in the middle between two adjacent bridges that cross them over the river, and area A is the farthest north of the beach. This results in the longer distance to the safe zone, which lead to the longer travel time. Without enough time to evacuate the hazard zone, they were caught in the tsunami.

Figure 4.11 presents the other extreme scenario, which shows the trajectories of the cars in case all the evacuees drive to a safe zone. One key difference between trajectories of pedestrians and trajectories of cars is that, unlike the cars, pedestrians can pass each other depending on their walking speeds. This means that the vehicles who make it to the transportation network later than the others are more likely to get stuck in congestion and get caught by the tsunami inundation. This explains why the red trajectories overlay the green curves. Looking at the trajectories of casualties, it can be observed that the agents who are located around the three main bridges (A, B and C) did not evacuate in time and get to the transportation network when it is congested and loaded, and thus caught by the tsunami on their way to shelters of D, E, and F.

Figure 4.12 shows the multi-modal evacuation trajectories (pedestrians and cars) with different splits of evacuation mode. The left column shows the pedestrian evacuees. It shows that the characteristics of trajectories do not change, except the density of pedestrians that increases from top to bottom. On the other hand, the distribution of casualties for cars changes dramatically as the percentage of them decreases. When 25% of evacuees drive, all of the cars evacuate safely to one of the shelters outside the hazard zone. While

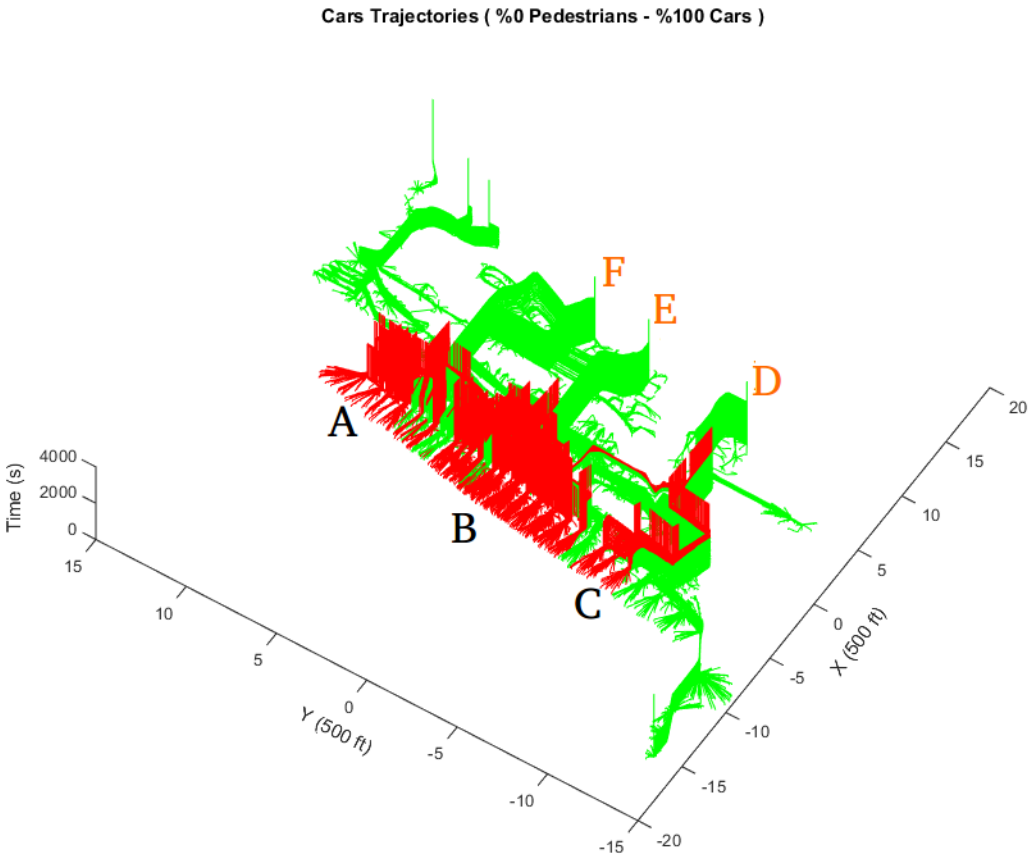

FIGURE 4.11: Car trajectories - 100% cars

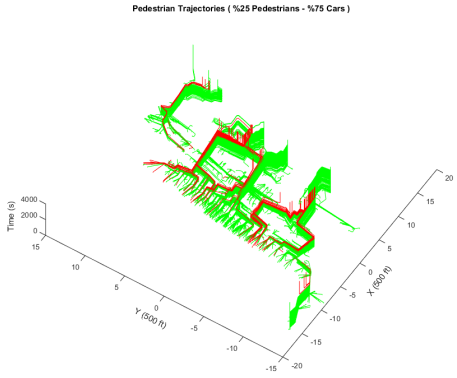

(a) Pedestrian trajectories (25% pedestrian)

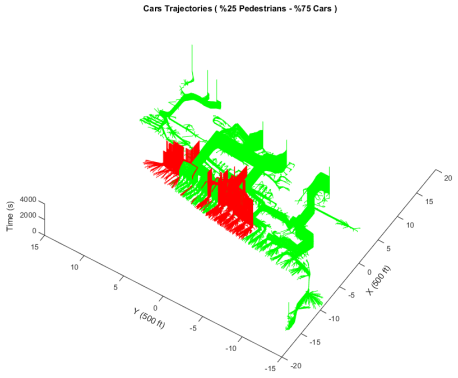

(b) Car trajectories (25% pedestrian)

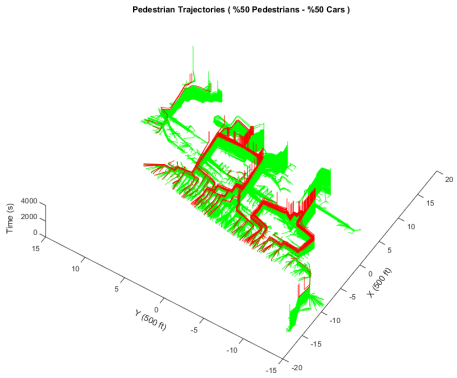

(c) Pedestrian trajectories (50% pedestrian)

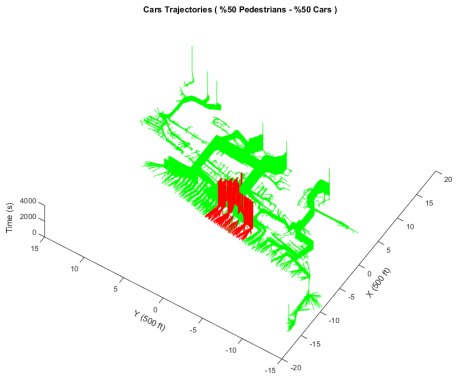

(d) Car trajectories (50% pedestrian)

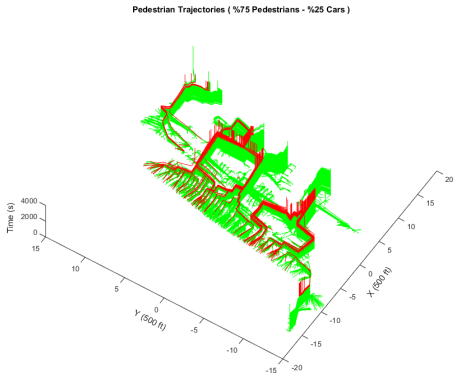

(e) Pedestrian trajectories (75% pedestrian)

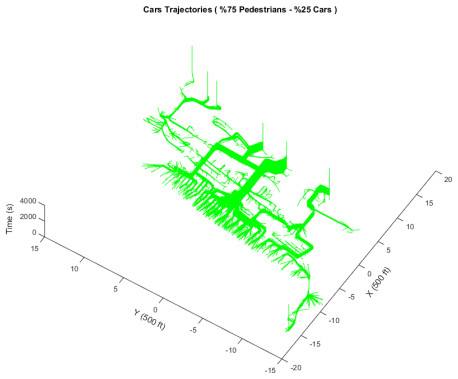

(f) Car trajectories (75% pedestrian)

FIGURE 4.12: Evacuation trajectories

in case of the 75% of evacuees drive, traffic congestion and bottleneck occurred on the top left bridge and the middle bridges causes a lot of fatalities in area A and B. In the scenario that evacuees choose to walk and percentage of vehicle drop to half of the population, congestion is no longer an issue for the north side of the beach, but a bottleneck is created in the downtown area still leads to high mortality rates for area B.

4.3. Summary

This section was dedicated to understanding the general behavior of evacuation and the influence of factors that affect the evacuation efficiency and the mortality rate of the scenario. The results have shown that mortality rate is highly correlated with the evacuation mode split, and there is an optimal split that leads to the lowest mortality rate, typically between 100% to 75% pedestrians. Likewise, minimum milling time strongly affects the number of fatalities, in a way that slight increase in τ can lead to significant increase in mortality rate, especially for the cases that the average walking speed of the community is low. Similarly, walking speed is of great importance for a successful evacuation, especially for higher milling times. Moreover, maximum driving speeds for pedestrians is influential under 20 mph. In addition, critical depth has shown less significance comparing to other factors. What's more, in this chapter, evacuation trajectories have been introduced to analyze the evacuation behavior and its travel patterns in 3-D visualization. It also facilitates the recognition of the critical spots and safe zones to optimize the evacuation strategies for different parts of the city. In the next chapter, we introduce a framework to systematically analyze transportation network and its vulnerability, recognize and identify the critical links of the network, and thus, to create an optimal retrofitting plan for the critical links of the network considering the limited amount of resources.

5. RESULTS: TRANSPORTATION NETWORK ASSESSMENT

Traditionally, critical link is identified through its contribution to the network travel time. In an evacuation scenario, however, life safety is the first priority. Building upon the agent-based tsunami evacuation platform, an innovative critical link identification method is presented in this chapter, along with the detailed retrofitting scheme which devotes to maximize the benefits of life safety.

5.1. Critical Links Identification

In this research, the criticality of a link comes from the impact of the failure of the link on life safety, and in particular mortality rates. It is, therefore, essential to identify all the critical links over the investigated transportation network. There are around 700 links within the transportation network of this case study, including bridges, streets, arterials, and highway links. The failure of all links, each at a time, have been assessed and the links that had the greatest impact on the mortality rate of evacuation scenario in the transportation network were identified. It is assumed that all the evacuees have prior knowledge regarding any broken links and reroute to their destination accordingly. To capture the variation of different decisions as well as walking speeds, each scenario has been simulated multiple times; the mean mortality of each scenario has been assessed to find critical links in the network. It is worth mentioning that, criticality of a link is correlated with the mode choice split. In other words, failure of a link can highly impact the efficiency of evacuation if the evacuees are evacuating on foot, but not in the case where evacuees drive, and vice versa. To account for different splits of evacuation mode, critical links have been identified for 5 different percentages of pedestrians and cars as following:

- 100% Pedestrians
- 75% Pedestrians - 25% Cars
- 50% Pedestrians - 50% Cars
- 25% Pedestrians - 75% Cars
- 100% Cars

Furthermore, this study focuses on the links that are considered critical among most of the cases, combined with engineering judgment and experts' opinions regarding the criticality of specific links in the network.

5.1.1 Critical Link Selection Criteria

Figure 5.1 shows the normalized increase in mortality rates of a scenario where a specific link is failed, over the average mortality rate of all links failures, for different evacuation mode splits. For example, looking at Figure 5.1(a), there are 10 links that their failure increases the mean mortality rate by at least 5%. Interestingly, there are a few links that are critical in cases where the majority of evacuees are pedestrians, but not in cases where the percentage of vehicles is high. Analogously, there are a few links that are considered as critical only when the percentage of cars is high. There are several links that are considered in all the evacuation mode splits. Figure 5.1(f) shows the average mortality rate increase for each link over all the 5 different evacuation mode splits. In this study, links which their failure causes an increase in mortality rate over 5% are considered as critical, and further assessment has been done on these identified links. The other links are expected to have minimal criticality and do not affect mortality rate dramatically upon failure as multiple alternative routes exist. In the next section, these critical links are mapped to the transportation network of Seaside to find the topographically and structurally critical ones to devise a retrofitting plan for.

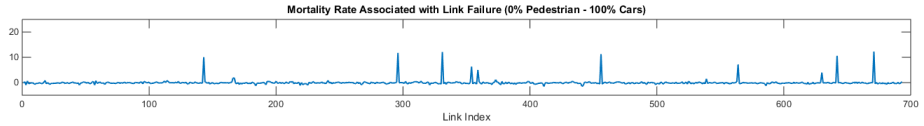

(a) 0% Pedestrain

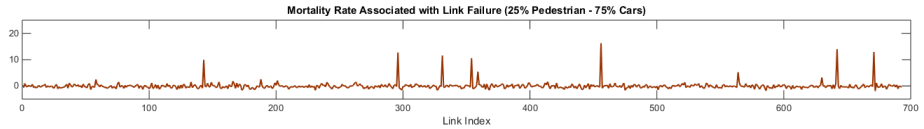

(b) 25% Pedestrain

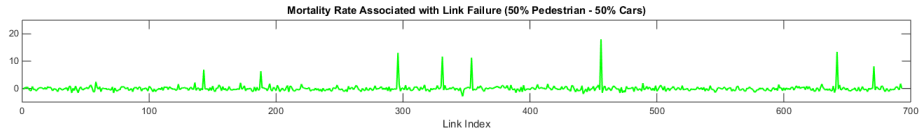

(c) 50% Pedestrain

(d) 75% Pedestrain

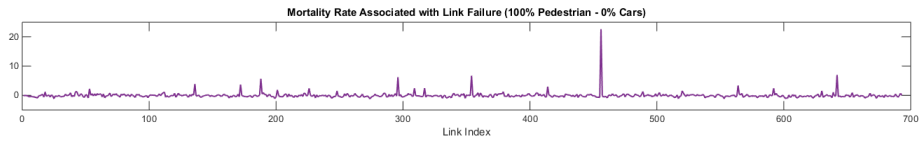

(e) 100% Pedestrain

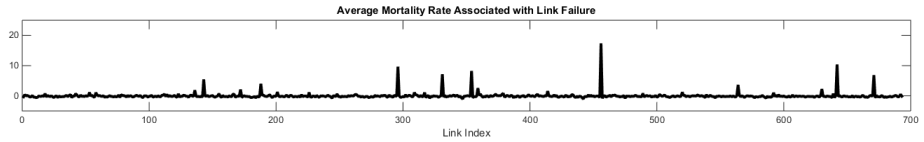

(f) Average

FIGURE 5.1: Normalized mortalities associated with each link's failure

5.1.2 Critical Links Visualization

Figure 5.3 shows the visualization of the identified critical links in the transportation network of this study for different evacuation mode choice combinations. Surprisingly, not all bridges have large impacts on mortality rates. It can be explained by the potential availability to alternative routes in case of failure. For high percentages of cars, Figures 5.2(a) and 5.2(b), four main bridges, and the roads leading to highly demanded shelters are marked as critical. This is mostly due to the fact that failure of either of these links causes a severe congestion to the other adjacent links, leading to higher travel times, and thus, higher fatality rates. As the percentage of vehicles decrease, the links which are adjacent to shelters are no longer marked as critical. Since although with the failure of those links, the evacuees are forced to choose another available shelter, the concentration of pedestrians does not have a huge impact on travel times as it does on vehicles. Therefore, as shown in figure 5.2(d) which represents the critical links for the evacuation scenario with 75% percent pedestrians and 25% cars, the critical links are narrowed down to three main bridges and one arterial which its failure cause an isolation to the top left part of the transportation network. For the scenario where all the evacuees decide to evacuate on foot, as in Figure 5.2(e), the bottom left road and its adjacent bridge is added to critical links. Mostly because their failure leads to a huge increase in distance to the safe zone for the agents in the lower parts of the beach. Figure 5.2(f) shows the critical links identified based on the average mortality increase over all the different mode splits.

In total, there are 13 critical links identified in the whole transportation network of Seaside, OR. However, not all of these links have equal impacts on mortality rate in an evacuation. Moreover, running retrofitting planning algorithm on 13 critical links is computationally expensive. Therefore, we have to narrow down the important links to the ones that are either known as being vulnerable or are expected to be influential on fatality rate with higher certainty. Since the four links in the far east side of the city, adjacent to

(a) 0% Pedestrain - 100% Cars

(b) 25% Pedestrain - 75% Cars

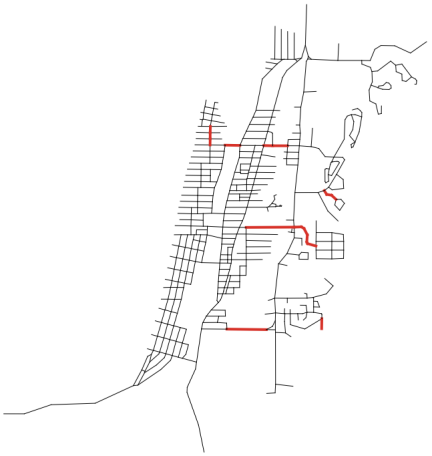

(c) 50% Pedestrain - 50% Cars

(d) 75% Pedestrain - 25% Cars

(e) 100% Pedestrain - 0% Cars

(f) Average

FIGURE 5.2: Color coded network, representing critical links

the evacuation shelters, locate outside of the inundation zone, retrofitting them does not seem to be of high priority. In addition, retrofitting arterials, compared to the bridges, is not of great significance since they are expected to be partially functional even facing extreme earthquakes. Even though they are closed for vehicles, they probably can still carry pedestrians. One exception, however, is the bottom left road which is highly prone to a landslide after an extreme earthquake. With all this in mind, and accounting for the insights of the structural engineers regarding the stability and vulnerability of the bridges and other links, there are five links identified for retrofitting purposes, shown in Figure 5.3. Further assessment of the degree to which a link is damaged in order to propose an optimal retrofitting plan is provided.

5.2. Retrofitting Analysis

In this section, we assess the damage to each of the previously determined critical links. Functionality states to which any transportation facility operates is categorized as follows:

1. Able to accommodate both vehicles and pedestrians (INTACT)
2. Able to accommodate only pedestrians (PED)
3. Not able to accommodate any kind of traffic (FAILED)

The goal is to prepare a retrofitting plan considering limited resources on the critical links to minimize mortality rates. Here are a few assumptions to devise a retrofitting plan:

- If a bridge is not retrofitted, it fails as a consequence of earthquake
- One level retrofitting costs one unit of resources and makes a bridge functional for pedestrians after earthquake

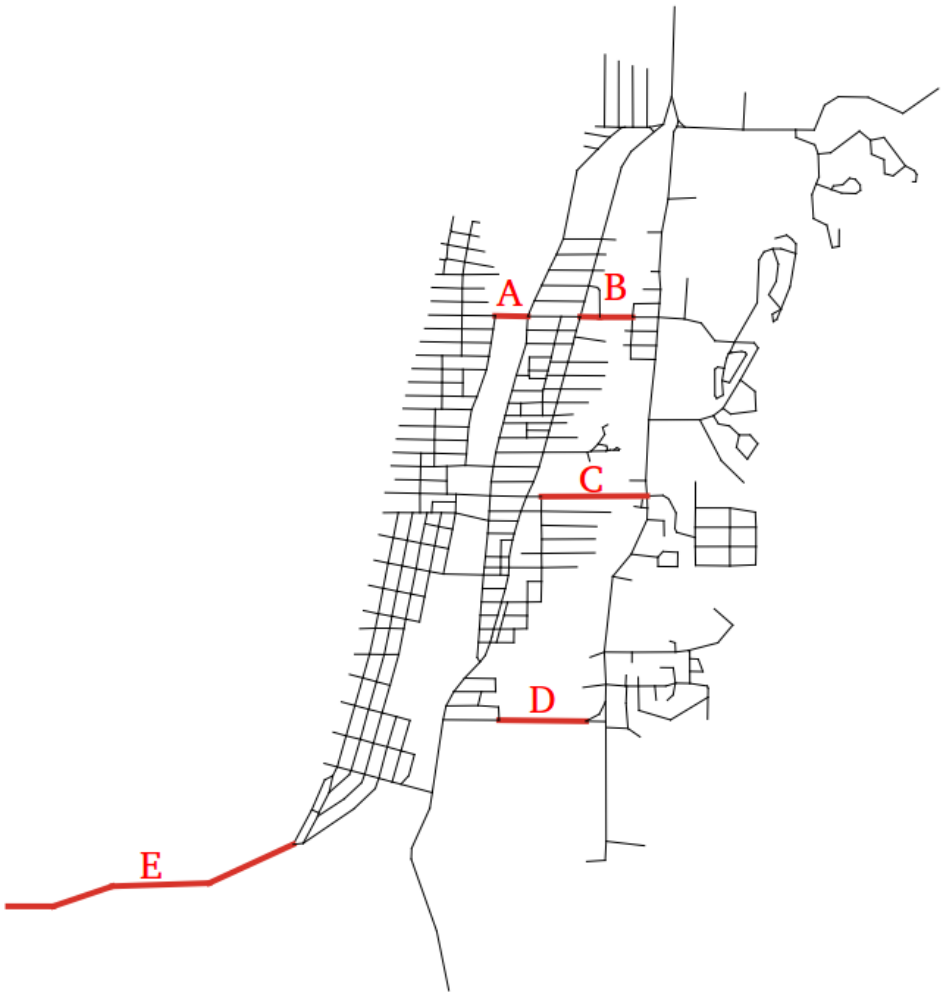

FIGURE 5.3: Final critical links

- Another level of retrofitting costs another $RATIO$ number of resources, and makes a bridge remain intact after the earthquake
- To fully retrofit a bridge, it costs $RATIO + 1$ number of resources

Considering the states mentioned, and for different values of $RATIO$ and splits of evacuation mode, retrofitting planning is represented in figures 5.4 through 5.5. Besides a detailed retrofitting plan for all the cases, the objective is to find general rules for retrofitting which can be applied to different evacuation cases with different splits and different retrofitting plans with different $RATIO$s. As expected, there are numerous ways to spend the few units of resources to retrofit the system. The aim is to minimize the mortality with respect to constraints on alternatives to spending those amount of resources. Following section explains a Constraint Satisfaction Problem that clears the limits and alternatives of spending a specific amount of resources.

5.2.1 Constraint Satisfaction Formulation

These alternatives can be formulated as a Constraint Satisfaction Problem (CSP):

$$N * 1 + M * (Ratio + 1) = R \tag{5.1}$$

$$N + M <= N_{cr} \tag{5.2}$$

$$N, M \in \mathbb{N} \tag{5.3}$$

Where,

N = Number of retrofitted links to be Pedestrian Accessible (PED)

M = Number of retrofitted links to be intact (INTACT)

R = Number of resources available

N_{cr} = Number of critical links (In our case, 5 links)

The above integer equation, can either have no integers answers for N and M, or have multiple sets of answers for N and M. After solving the above equation, the number of alternatives ($N_{alternatives}$) to spend R number of resources on $M + N$ bridges can be calculated as following:

$$N_{alternatives} = \sum_{M,N} \binom{N_{cr}}{M+N} \binom{M+N}{M} \tag{5.4}$$

As shown in figures, the blue dots represent mean mortality rates associated with the various resource consumption alternatives from retrofitting. For example, if we assume the $RATIO = 2$, and we have $R = 6$ number of resources, considering city of Seaside, with $N_{cr} = 5$ identified critical links, the solutions to equation 5.1 would be as following,

- $N = 0$ and $M = 2$, Retrofiring two bridges to the highest extent (INTACT)
- $N = 3$ and $M = 1$, Retrofitting one of the bridges to the highest extent (INTACT) and two of the others to be pedestrian accessible (PED)

In light of equation 5.4, number of different alternatives for spending 6 resources with above combination on 5 critical links can be calculated as following,

$$N_{alternatives} = \binom{5}{2}\binom{2}{0} + \binom{5}{4}\binom{4}{1} = 10 + 20 = 30$$

As Figure 5.4(b) through 5.5(b) shows, 30 blue dots for $R = 6$ are plotted which represent the mortality rates associated with 30 different alternatives of spending 6 amount of resources.

5.2.2 Retrofitting Scheme

Figures 5.4 through 5.5 represent the expected mortality rate associated with different alternatives of spending different amount of resources. As stated in the objective,

for each specific amount of resources, the alternative that leads to the lowest mortality rate is the best option and it is represented by the green line in figures. Moreover, the red line represents the upper bound of spending specific resources. In other words, it bounds the worst option of spending a specific amount of resources which results in the highest mortality rate. As before, to capture the stochasticity of the system, each scenario has been simulated multiple times and mean mortality rates were used for assessment. The slopes of green lines between resource units represent the value of the retrofitting in terms of decreasing mortality rates. In other words, this can be translated into a cost-benefit problem in which one considers the cost of retrofitting and consuming resources against the benefit of decreasing the number of fatalities.

Retrofitting, in rare cases, can surprisingly increase the mortality rate. This phenomenon happens mostly due to opening a new route to cars that may result in concentrations of vehicles. In these cases, road closure (e.g. network disruption) will result in dissipation of traffic that leads to lower densities, and thus, lower travel times. However, the availability of a major route for vehicles might encourage a rebound effect in which additional people decide to use the link, which in turn causes severe congestion and higher travel times.

Single Mode Evacuation

Figure 5.4 shows the retrofitting benefits for the case that none of the evacuees walk and all the population drive to safe zones. In this case, we see that parameter $RATIO$ has no impact on the details of retrofitting plans since there are no pedestrians using the network, and thus, retrofitting a bridge to stay pedestrian accessible has no impact on the mortality rate. It can also be seen that retrofitting the first bridge to remain INTACT has the most value and decreases the mortality rate by 25%. Table 5.1 shows the priority of critical links to be retrofitted.

Figure 5.5 shows the benefit of retrofitting links in the case that all the evacuees

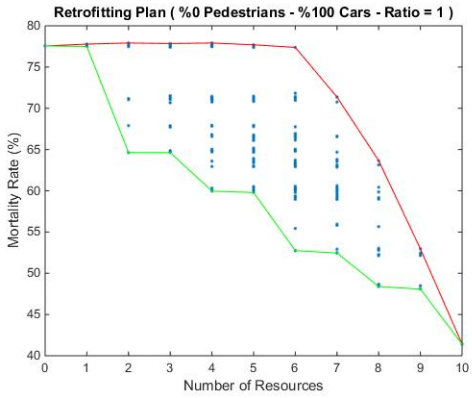

(a) Ratio = 1

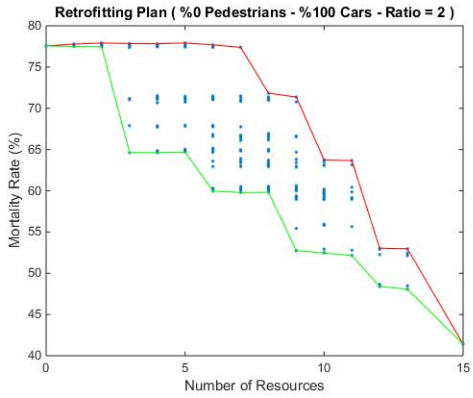

(b) Ratio = 2

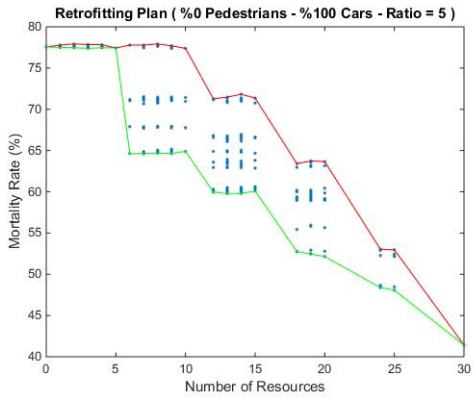

(c) Ratio = 5

FIGURE 5.4: Retrofitting resources planning - 0% pedestrian

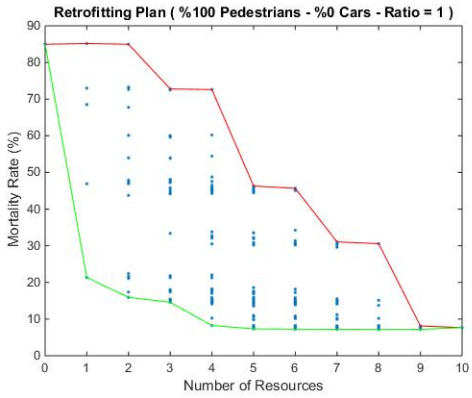

(a) Ratio = 1

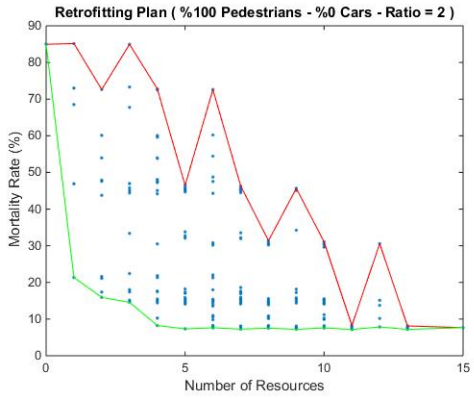

(b) Ratio = 2

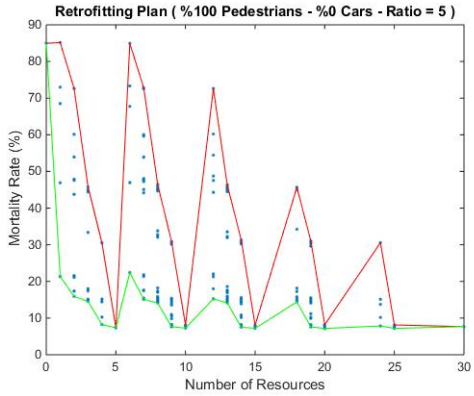

(c) Ratio = 5

FIGURE 5.5: Retrofitting resources planning - 100% pedestrian

evacuate on foot. Therefore, there would be no benefit in retrofitting a link to remain INTACT since there are no cars using the network. This explains the green curve in the figures to decrease in the beginning and stays the same as the bridges are upgraded to remain INTACT. Like the other single mode evacuation case, retrofitting the first bridge has the most value and decreases the mortality rate by 65%. Table 5.1 shows the priority of critical links to be retrofitted.

TABLE 5.1: Retrofitting plan details - single mode evacuation

Number of Retrofitted Links	Pedestrian (%)	Critical Link					Mortality Rate (%)
		A	B	C	D	E	
1	0	FAILED	FAILED	FAILED	FAILED	INTACT	64.63
	100	FAILED	FAILED	PED	FAILED	FAILED	21.33
2	0	FAILED	FAILED	INTACT	INTACT	FAILED	59.96
	100	FAILED	FAILED	PED	FAILED	PED	15.93
3	0	FAILED	FAILED	INTACT	INTACT	INTACT	52.74
	100	FAILED	FAILED	PED	PED	PED	14.57
4	0	FAILED	INTACT	INTACT	INTACT	INTACT	48.39
	100	PED	PED	PED	FAILED	PED	8.24
5	0	INTACT	INTACT	INTACT	INTACT	INTACT	41.41
	100	PED	PED	PED	PED	PED	7.33

Looking at Table 5.1, the first link that should be retrofitted for cars is Link E which helps to evacuate all the cars that are on the west side of the city and the beach area to the bottom left evacuation shelters. Retrofitting Bridge C by itself does not have a significant impact on the mortality rate for cars since it does not provide enough capacity for all the evacuees who are located on the beach to evacuate to the east side shelters. On the other hand, in the case of evacuation on foot, retrofitting bridge C has the higher impact and helps people move to safe zones quicker. The rest of the retrofitting priorities for these two cases can easily be interpreted by the table.

Multi-modal Evacuation

Figures 5.6 through 5.8 shows the decrease in expected mortality rate when the evacuation is multi-modal. Analogously, it can be interpreted as described in single model evacuation.

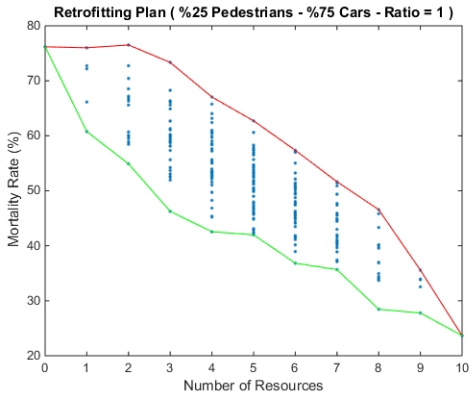

(a) Ratio = 1

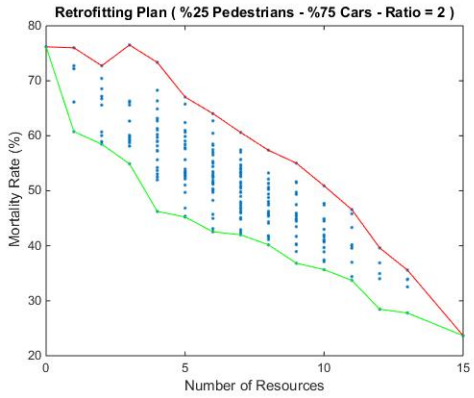

(b) Ratio = 2

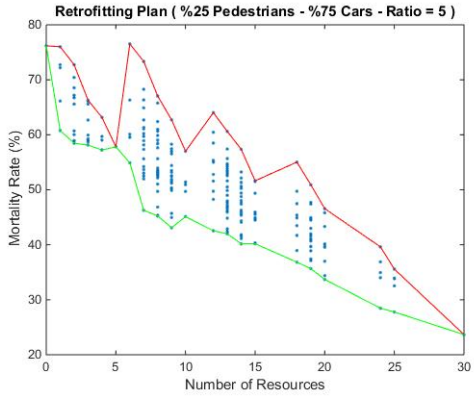

(c) Ratio = 5

FIGURE 5.6: Retrofitting resources planning - 25% pedestrian

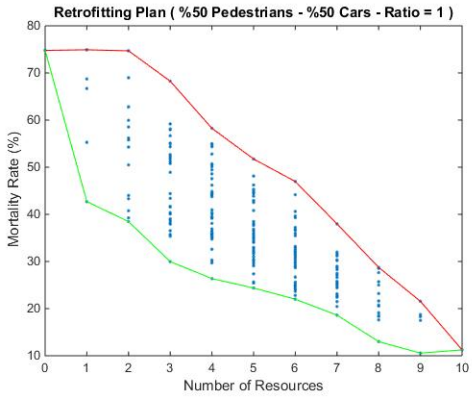

(a) Ratio = 1

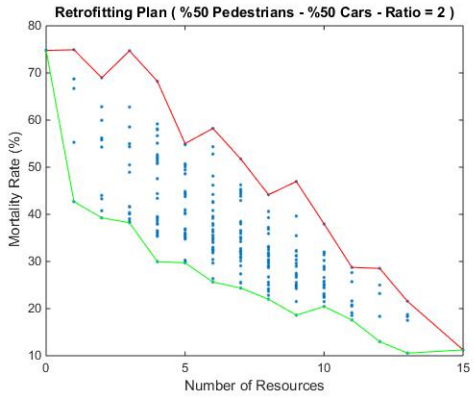

(b) Ratio = 2

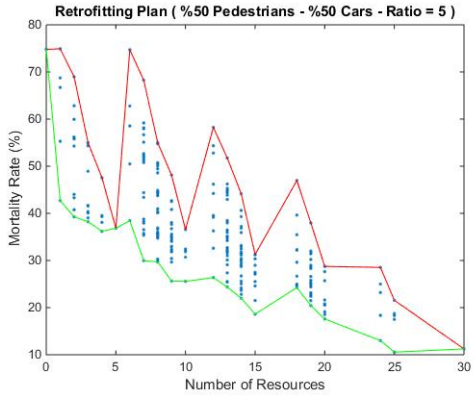

(c) Ratio = 5

FIGURE 5.7: Retrofitting resources planning - 50% pedestrian

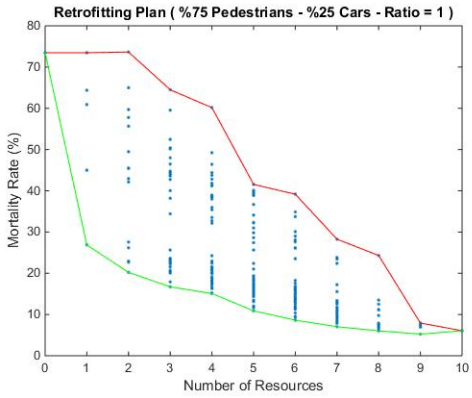

(a) Ratio = 1

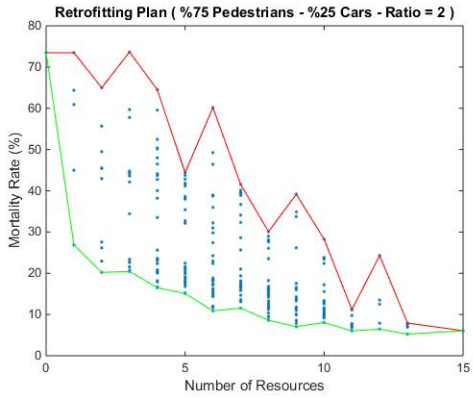

(b) Ratio = 2

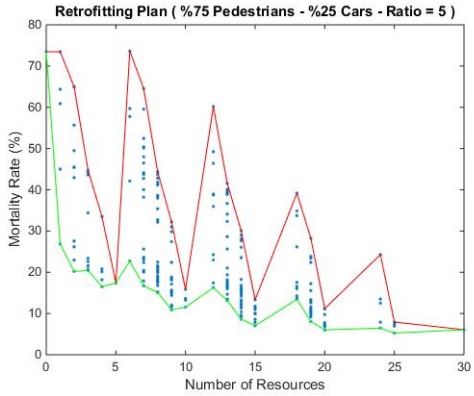

(c) Ratio = 5

FIGURE 5.8: Retrofitting resources planning - 75% pedestrian

TABLE 5.2: Retrofitting plan details - multi-modal evacuation - $RATIO = 1$

Number of Resources	Pedestrian (%)	Critical Link					Motality Rate (%)
		A	B	C	D	E	
1	25	FAILED	FAILED	PED	FAILED	FAILED	60.76
	50	FAILED	FAILED	PED	FAILED	FAILED	42.70
	75	FAILED	FAILED	PED	FAILED	FAILED	26.86
2	25	FAILED	FAILED	INTACT	FAILED	FAILED	54.90
	50	FAILED	FAILED	INTACT	FAILED	FAILED	38.46
	75	FAILED	FAILED	PED	FAILED	PED	20.22
3	25	FAILED	FAILED	PED	FAILED	INTACT	46.26
	50	FAILED	FAILED	PED	FAILED	INTACT	29.97
	75	FAILED	FAILED	PED	FAILED	INTACT	16.71
4	25	FAILED	FAILED	INTACT	INTACT	FAILED	42.55
	50	FAILED	FAILED	INTACT	INTACT	FAILED	26.37
	75	FAILED	PED	PED	FAILED	INTACT	15.09
5	25	FAILED	FAILED	INTACT	INTACT	PED	41.99
	50	FAILED	INTACT	PED	INTACT	FAILED	24.37
	75	PED	PED	PED	FAILED	INTACT	10.89
6	25	FAILED	FAILED	INTACT	INTACT	INTACT	36.84
	50	PED	INTACT	PED	INTACT	FAILED	22.00
	75	PED	INTACT	PED	INTACT	FAILED	8.62
7	25	FAILED	INTACT	PED	INTACT	INTACT	35.66
	50	PED	INTACT	PED	INTACT	PED	18.62
	75	PED	INTACT	PED	INTACT	PED	7.04
8	25	INTACT	INTACT	INTACT	INTACT	FAILED	28.46
	50	INTACT	INTACT	INTACT	INTACT	FAILED	13.00
	75	INTACT	INTACT	PED	INTACT	PED	6.02
9	25	INTACT	INTACT	INTACT	INTACT	PED	27.77
	50	INTACT	INTACT	INTACT	INTACT	PED	10.55
	75	INTACT	INTACT	INTACT	INTACT	PED	5.24

TABLE 5.3: Retrofitting plan details - multi-modal evacuation - $RATIO = 2$

Number of Resources	Pedestrian (%)	Critical Link					Mortality Rate (%)
		A	B	C	D	E	
1	25	FAILED	FAILED	PED	FAILED	FAILED	60.76
	50	FAILED	FAILED	PED	FAILED	FAILED	42.70
	75	FAILED	FAILED	PED	FAILED	FAILED	26.86
2	25	FAILED	FAILED	PED	FAILED	PED	58.48
	50	FAILED	FAILED	PED	FAILED	PED	39.26
	75	FAILED	FAILED	PED	FAILED	PED	20.22
3	25	FAILED	FAILED	INTACT	FAILED	FAILED	54.90
	50	PED	PED	PED	FAILED	FAILED	38.21
	75	PED	PED	PED	FAILED	FAILED	20.44
4	25	FAILED	FAILED	PED	FAILED	INTACT	46.26
	50	FAILED	FAILED	PED	FAILED	INTACT	29.97
	75	PED	PED	PED	FAILED	PED	16.51
5	25	FAILED	PED	PED	FAILED	INTACT	45.23
	50	FAILED	PED	PED	FAILED	INTACT	29.70
	75	FAILED	PED	PED	FAILED	INTACT	15.09
6	25	FAILED	FAILED	INTACT	INTACT	FAILED	42.55
	50	PED	PED	PED	FAILED	INTACT	25.64
	75	PED	PED	PED	FAILED	INTACT	10.89
7	25	FAILED	FAILED	INTACT	INTACT	PED	41.99
	50	FAILED	INTACT	PED	INTACT	FAILED	24.37
	75	PED	PED	PED	PED	INTACT	11.53
8	25	PED	INTACT	PED	INTACT	FAILED	40.17
	50	PED	INTACT	PED	INTACT	FAILED	22.00
	75	PED	INTACT	PED	INTACT	FAILED	8.62
9	25	FAILED	FAILED	INTACT	INTACT	INTACT	36.84
	50	PED	INTACT	PED	INTACT	PED	18.62
	75	PED	INTACT	PED	INTACT	PED	7.04
10	25	FAILED	INTACT	PED	INTACT	INTACT	35.66
	50	PED	INTACT	INTACT	INTACT	FAILED	20.44
	75	INTACT	INTACT	PED	INTACT	FAILED	8.06
11	25	PED	INTACT	PED	INTACT	INTACT	33.70
	50	PED	INTACT	PED	INTACT	INTACT	17.60
	75	INTACT	INTACT	PED	INTACT	PED	6.02
12	25	INTACT	INTACT	INTACT	INTACT	FAILED	28.46
	50	INTACT	INTACT	INTACT	INTACT	FAILED	13.00
	75	INTACT	INTACT	INTACT	FAILED	INTACT	6.47
13	25	INTACT	INTACT	INTACT	INTACT	PED	27.77
	50	INTACT	INTACT	INTACT	INTACT	PED	10.55
	75	INTACT	INTACT	INTACT	INTACT	PED	5.24
15	25	INTACT	INTACT	INTACT	INTACT	INTACT	23.66
	50	INTACT	INTACT	INTACT	INTACT	INTACT	11.24
	75	INTACT	INTACT	INTACT	INTACT	INTACT	6.07

TABLE 5.4: Retrofitting plan details - multi-modal evacuation - $RATIO = 5$

Number of Resources	Pedestrian (%)	Critical Link					Mortality Rate (%)
		A	B	C	D	E	
1	25	FAILED	FAILED	PED	FAILED	FAILED	60.76
	50	FAILED	FAILED	PED	FAILED	FAILED	42.70
	75	FAILED	FAILED	PED	FAILED	FAILED	26.86
2	25	FAILED	FAILED	PED	FAILED	PED	58.48
	50	FAILED	FAILED	PED	FAILED	PED	39.26
	75	FAILED	FAILED	PED	FAILED	PED	20.22
3	25	FAILED	PED	PED	FAILED	PED	58.12
	50	PED	PED	PED	FAILED	FAILED	38.21
	75	PED	PED	PED	FAILED	FAILED	20.44
4	25	PED	PED	PED	FAILED	PED	57.23
	50	PED	PED	PED	FAILED	PED	36.19
	75	PED	PED	PED	FAILED	PED	16.51
5	25	PED	PED	PED	PED	PED	57.81
	50	PED	PED	PED	PED	PED	36.84
	75	PED	PED	PED	PED	PED	17.40
6	25	FAILED	FAILED	INTACT	FAILED	FAILED	54.90
	50	FAILED	FAILED	INTACT	FAILED	FAILED	38.46
	75	FAILED	FAILED	INTACT	FAILED	FAILED	22.68
7	25	FAILED	FAILED	PED	FAILED	INTACT	46.26
	50	FAILED	FAILED	PED	FAILED	INTACT	29.97
	75	FAILED	FAILED	PED	FAILED	INTACT	16.71
8	25	FAILED	PED	PED	FAILED	INTACT	45.23
	50	FAILED	PED	PED	FAILED	INTACT	29.70
	75	FAILED	PED	PED	FAILED	INTACT	15.09
9	25	PED	PED	PED	FAILED	INTACT	43.10
	50	PED	PED	PED	FAILED	INTACT	25.64
	75	PED	PED	PED	FAILED	INTACT	10.89
10	25	PED	PED	PED	PED	INTACT	45.12
	50	PED	PED	PED	PED	INTACT	25.57
	75	PED	PED	PED	PED	INTACT	11.53
12	25	FAILED	FAILED	INTACT	INTACT	FAILED	42.55
	50	FAILED	FAILED	INTACT	INTACT	FAILED	26.37
	75	FAILED	FAILED	INTACT	INTACT	FAILED	16.29
13	25	FAILED	FAILED	INTACT	INTACT	PED	41.99
	50	FAILED	INTACT	PED	INTACT	FAILED	24.37
	75	FAILED	INTACT	PED	INTACT	FAILED	13.13
14	25	PED	INTACT	PED	INTACT	FAILED	40.17
	50	PED	INTACT	PED	INTACT	FAILED	22.00
	75	PED	INTACT	PED	INTACT	FAILED	8.62
15	25	PED	PED	INTACT	INTACT	PED	40.19
	50	PED	INTACT	PED	INTACT	PED	18.62
	75	PED	INTACT	PED	INTACT	PED	7.04
18	25	FAILED	FAILED	INTACT	INTACT	INTACT	36.84
	50	FAILED	INTACT	INTACT	INTACT	FAILED	24.26
	75	FAILED	FAILED	INTACT	INTACT	INTACT	13.42
19	25	FAILED	INTACT	PED	INTACT	INTACT	35.66
	50	PED	INTACT	INTACT	INTACT	FAILED	20.44
	75	INTACT	INTACT	PED	INTACT	FAILED	8.06
20	25	PED	INTACT	PED	INTACT	INTACT	33.70
	50	PED	INTACT	PED	INTACT	INTACT	17.60
	75	INTACT	INTACT	PED	INTACT	PED	6.02
24	25	INTACT	INTACT	INTACT	INTACT	FAILED	28.46
	50	INTACT	INTACT	INTACT	INTACT	FAILED	13.00
	75	INTACT	INTACT	INTACT	FAILED	INTACT	6.47
25	25	INTACT	INTACT	INTACT	INTACT	PED	27.77
	50	INTACT	INTACT	INTACT	INTACT	PED	10.55
	75	INTACT	INTACT	INTACT	INTACT	PED	5.24

In addition, Tables 5.2 through 5.4 present the retrofitting plan's details for multi-modal evacuation with different retrofitting $RATIO$s. For example, if the retrofitting $RATIO$ equals to 2 and the amount of available resources is 6, using Table 5.3, we can see that the optimal retrofitting option is as following:

- 25% Pedestrian - 75% Cars: Bridges C and D should be intact (INTACT)
- 50% Pedestrian - 50% Cars: Bridges A, B, and C should be pedestrian accessible (PED) and Link E should be intact (INTACT).
- 75% Pedestrian - 25% Cars: Bridges A, B, and C should be pedestrian accessible (PED) and Link E should be intact (INTACT).

This is mostly because as the percentage of the pedestrians increases, having INTACT bridges loses its importance. Therefore, the rational decision would be to distribute the resources in a way to have more pedestrian accessible links and bridges.

Looking at Tables 5.2 to 5.4, it can be interpreted that in almost all of the cases, Bridge C is the first one that should be retrofitted, followed by Link E, Bridge B, and Bridge D. Among these 5 critical links, Bridge A has is almost the last one to be retrofitted in most of the cases.

5.3. Summary

In this chapter, we introduced a framework to systematically identify, recognize, and mark the critical links of the transportation network, which their failure severely impacts the mortality rate of the scenario and the efficiency of the evacuation. Critical links have been marked for different evacuation mode splits since one link can be highly influential when one of the evacuation modes has the majority, but not when the other mode rules. After that, a mutual set of critical links of all the evacuation mode splits, informed by

the engineering judgment and structural criticality and vulnerability of the link, has been chosen for further retrofitting assessment. Then a retrofitting plan has been devised to minimize the number of fatalities considering the limited amount of resources. The analysis took into consideration different levels of retrofitting (i.e., Pedestrian Accessible and Intact). The results of the assessment of Seaside transportation network has shown that neither all the bridges failure impact the mortality rate, nor all the critical links are the bridges. Furthermore, retrofitting schemes have shown that in most of the cases, Bridge C has the highest priority to be retrofitted, and after that, depending on the mode choice split, link E, bridge D, or bridge B are the most important ones. Bridge A has the lowest priority in almost all the cases.

6. DISCUSSION AND CONCLUSION

6.1. Summary

This research presented a near-field multi-modal tsunami evacuation study through an agent-based modeling environment. The research questions were how variations in decision-making time (i.e., τ and σ), choices of transportation modes, and in general influential factors in an evacuation scenario impact the coastal community life safety (i.e., mortality rate), using Seaside, Oregon as a case study. An agent-based modeling environment, NetLogo, was used to model and assess the sensitivity of mortality rate to the factors involved in the evacuation scenario. The results show that (1) the mortality rate is sensitive to the decision-making time τ which is a "delay time" or "milling time" (2) walking speed has significant impacts on the estimation of the number of fatalities; (3) maximum driving speed is also influential for the speed limits lower than 20 mph; and (4) the mortality rate is highly correlated with evacuation mode choice, in a way that there is an optimal mode split that leads to the lowest mortality rates and is typically towards the evacuation on foot.

In addition, this work implemented an agent-based modeling approach to investigate the criticality of transportation network links for an emergency multi-modal evacuation scenario. The mortality rate has been analyzed to mark the state of criticality of a link. The results show that neither all the most used links nor all the initially expected important links throughout the networks are critical. The criticality of a link is assessed by the impact of the particular link's failure on the mortality rate of the scenario. The idea has been applied to the City of Seaside, OR, and results lead to marking 4 bridges and 1 link as critical, whose failure each increases the mortality rates by great amounts. Further analysis has been done on these so-called "severely critical" links. The links were

set to have three different stages: (1) Both Pedestrian and Car accessible (INTACT), (2) Pedestrian Accessible Only (PED), and (3) Collapsed (FAILED). Assuming different retrofitting RATIOs, an optimal retrofitting plan has been suggested to minimize the number of fatalities at each time period considering the limited resources. This idea also captures the marginal mortality rate with the change in number of resources available to provide a base to assess further cost-benefit analyses.

6.2. Future Work

The presence of vertical evacuation shelters can severely change the criticality of a link. At some point, investing resources on building highly resistant shelter structures inside the inundation zone might be more economical than spending greater amounts of resources on retrofitting bridges or transportation links. Therefore, future work will incorporate the impact of having vertical evacuation shelters on vulnerability and criticality of transportation systems. In addition, social aspects of the evacuation scenario necessitates more extensive investigation. Coalescing behavior, car-abandoning (evacuation mode transfer) and communications (information provision and propagation strategies) must be considered in a realistic evacuation platform. Moreover, in some cases, damage may reduce the capacity of the facility, but not to an extent in which only pedestrians can pass through. Thus, capacity drop, as a consequence of earthquake damage to the transportation network, may be a better metric for assessment. In addition, realistic interaction rules among agents (i.e., pedestrian and car interaction) to provide more accurate representation of the multimodal evacuation should be taken into consideration. Population distribution has also great impact on the mortality rate, and analyzing different population distributions reflecting day-time or night-time can be beneficial to this study.

BIBLIOGRAPHY

Akiyama, M., Frangopol, D. M., Arai, M., Koshimura, S., March 2012. Probabilistic assessment of structural performance of bridges under tsunami hazard. ASCE Structures Congress, 1919–1928.

Almeida, J. E., Rosseti, R. J., Coelho, A. L., 2013. Crowd simulation modeling applied to emergency and evacuation simulations using multi-agent systems. arXiv preprint arXiv:1303.4692.

Assaf, H., 2011. Framework for modeling mass disasters. Natural Hazards Review 12 (2), 47–61.

Balakrishna, R., Wen, Y., Ben-Akiva, M., Antoniou, C., 2008. Simulation-based framework for transportation network management in emergencies. Transportation Research Record: Journal of the Transportation Research Board (2041), 80–88.

Berdica, K., 2002. An introduction to road vulnerability: what has been done, is done and should be done. Transport Policy 9 (2), 117–127.

Bocchini, P., Frangopol, D. M., 2010. Optimal resilience-and cost-based postdisaster intervention prioritization for bridges along a highway segment. Journal of Bridge Engineering 17 (1), 117–129.

Bonabeau, E., 2002. Agent-based modeling: Methods and techniques for simulating human systems. Proceedings of the National Academy of Sciences 99 (suppl 3), 7280–7287.

Chalmet, L. G., Francis, R. L., Saunders, P. B., 1982. Network models for building evacuation. Management science 28 (1), 86–105.

Chang, L., Peng, F., Ouyang, Y., Elnashai, A. S., Jr, B. F. S., 2012. Bridge seismic retrofit

program planning to maximize postearthquake transportation network capacity. Journal of Infrastructure Systems 18 (2), 75–88.

Chen, X., Zhan, F. B., 2006. Agent-based modelling and simulation of urban evacuation: relative effectiveness of simultaneous and staged evacuation strategies. Journal of the Operational Research Society 59 (1), 25–33.

Dawson, R. J., Peppe, R., Wang, M., 2011. An agent-based model for risk-based flood incident management. Natural hazards 59(1), 167–189.

Earnest, D. C., 2011. Geographic distribution of disruptions in weighted complex networks: An agent-based model of the us air transportation network. AAAI Fall Symposium: Complex Adaptive Systems, 34–43.

FEMA, June 2008. Guidelines for design of structures for vertical evacuation from tsunamis. Technical report, APPLIED TECHNOLOGY COUNCIL, 201 Redwood Shores Pkwy, Suite 240 Redwood City, California 94065.

Franzese, O., Han, L., 2001. Traffic modeling framework for hurricane evacuation. Internal report, Oak Ridge National Laboratory.

Goldfinger, C., Nelson, C. H., Morey, A. E., Johnson, J. E., Patton, J. R., Karabanov, E., e. a., 2012. Turbidite event historymethods and implications for holocene paleoseismicity of the cascadia subduction zone. U.S. Geological Survey Professional Paper 1661F, 170.

Hamacher, H. W., Tjandra, S. A., 2002. Mathematical modelling of evacuation problems-a state of the art. Pedestrian and Evacuation Dynamics 24, 227–266.

Hobeika, A. G., Jamei, B., 1985. Massvac: A model for calculating evacuation times under natural disasters. Emergency Planning, 23–28.

Hobeika, A. G., Kim, S., Beckwith, R. E., 1994. A decision support system for developing evacuation plans around nuclear power stations. Interfaces 24(5), 22–35.

Jafari, M., Bakhadyrov, I., Maher, A., 2003. Technological advances in evacuation planning and emergency management: current state of the art. Rutgers University, Center for Advanced Infrastructure & Transportation (EVAC-RU4474).

Jenelius, E., Mattsson, L.-G., 2012. Road network vulnerability analysis of area-covering disruptions: A grid-based approach with case study. Transportation research part A: policy and practice 46 (5), 746–760.

Jenelius, E., Mattsson, L.-G., Levinson, D., 2010. The traveler costs of unplanned transport network disruptions: An activity-based modeling approach (201104), 1–34.

Jonkman, S. N., Vrijling, J., Vrouwenvelder, A. C. W. M., 2008. Methods for the estimation of loss of life due to floods: A literature review and a proposal for a new method. Natural Hazards 46, 353389.

Kang, J.E., M. L., Prater., C., 2004. Hurricane evacuation expectations and actual behavior in hurrican lili. Tech. rep., College Station, TX: Texas A & M University Hazard Reduction and Recovery Center.

Katada, T., Kuwasawa, N., Yeh, H., Pancake, C., 2006. Integrated simulation of tsunami hazards. In: In 100th Anniversary Earthquake Conference including the 8th U.S. National Conference on Earthquake Engineering (8NCEE), the SSA Centennial Meeting, and the OES Disaster Resistant California Conference,. No. 1727. San Francisco, California.

Kiremidjian, A., Moore, J., Fan, Y. Y., Yazlali, O., Basoz, N., Williams, M., 2007. Seismic risk assessment of transportation network systems. Journal of Earthquake Engineering 11 (3), 371–382.

KLD, 1984. Formulations of the dynev and i-dynev traffic simulation models used in

esf. Technical report prepared for the Federal Emergency Management Agency, KLD Associates, Washington, DC.

Klugl, F., Bazzan, A. L. C., 2012. Agent-based modeling and simulation. AI Magazine, 29–40.

Klunder, G., Terbruggen, E., Mak, J., Immers, B., 2009. Large-scale evacuation of the randstad evacuation simulations with the dynamic traffic assignment model indy. Proceedings of the 1st International Conference on Evacuation Modeling and Management.

Knoblauch, R., Pietrucha, M., Nitzburg, M., TRB, National Research Council, Washington, DC, pp 1995. Field studies of pedestrian walking speed and start-up time. Transportation Research Record 1538, 2738.

Konduri, K. C., Pendyala, R. M., You, D., Chiu, Y.-C., Hickman, M., Noh, H., Gardner, B., Waddell, P., Wang, L., 2013. A network-sensitive transport modeling framework for evaluating impacts of network disruptions on traveler choices under varying levels of user information provision. 92nd Annual Meeting of the Transportation Research Board, Washington, DC 510.

Koshimura, S., Katada, T., Mofjeld, H. O., Kawata, Y., 2006. A method for estimating casualties due to the tsunami inundation flow. Natural Hazards 39(2), 265–274.

Kwon, E., Pitt, S., 2005. Evaluation of emergency evacuation strategies for downtown event traffic using a dynamic network model. Transportation Research Record: Journal of the Transportation Research Board (1922), 145–199.

Lammel, G., 2011. Escaping the tsunami: Evacuation strategies for large urban areas concepts and implementation of a multi-agent based approach. Ph.D. thesis, Universitatsbibliothek.

Lindell, M. K., Prater, C. S., 2007. Critical behavioral assumptions in evacuation time estimate analysis for private vehicles: Examples from hurricane research and planning. Journal of Urban Planning and Development 133 (1), 1829.

Liu, H. X., Ban, J. X., Ma, W., Mirchandani, P. B., 2007. Model reference adaptive control framework for real-time traffic management under emergency evacuation. Journal of Urban Planning and Development 133 (1), 43–50.

Liu, Y., Okada, N., Takeuchi, Y., 2009. Dynamic route decision model-based multi-agent evacuation simulation - case study of nagata ward, kobe. Journal of Natural Disaster Science 28(2), 91–98.

Lovs, G. G., 1998. Models of wayfinding in emergency evacuations. European journal of operational research 105 (3), 371–389.

Mas, E., Imamura, F., Koshimura, S., 2011. Modeling the decision of evacuation from tsunami, based on human risk perception. In: In Annual Meeting of the Tohoku Branch Technology Research Conference. Japan Society of Civil Engineers.

Mas, E., Suppasri, A., Imamura, F., Koshimura, S., 2012. Agent-based simulation of the 2011 great east japan earthquake/tsunami evacuation: An integrated model of tsunami inundation and evacuation. Journal of Natural Disaster Science 34 (1), 41–57.

Mas, Erick, F. I., Koshimura., S., 2012. An agent-based model for the tsunami simulation: Case study of the 2011 great east japan tsunami in arahama town. In: Joint Conference Proceeding. 9th International Conference on Urban Earthquake Engineering & 4th Asia Conference on Earthquake Engineering. Tokyo Institute of Technology, Tokyo, Japan.

Mas, Erick, I. F., Koshimura, S., 2012. An agent based model for tsunami evacuation simulation. a case study of the 2011 great east japan tsunami in arahama town. In:

in: Joint conference proceedings of 9th international conference on urban earthquake engineering and 4th Asia conference on earthquake engineering, Tokyo, March 6-8.

Miller, H. J., Wu, Y.-H., Hung, M.-C., 1999. Gis-based dynamic traffic congestion modeling to support time-critical logistics. Systems Sciences, 1999. HICSS-32. Proceedings of the 32nd Annual Hawaii International Conference on.

Murray-Tuite, P., 2007. Perspectives for network management in response to unplanned disruptions. Journal of urban planning and development 133 (1), 9–17.

Murray-Tuite, P., Mahmassani, H. S., 2005. Identification of vulnerable transportation infrastructure and household decision making under emergency evacuation conditions. No. SWUTC/05/167528-1, Southwest Region University Transportation Center, Center for Transportation Research, University of Texas at Austin.

Nagarajan, M., Shaw, D., Albores, P., August 2012. Disseminating a warning message to evacuate: A simulation study of the behaviour of neighbours. European Journal of Operational Research 220 (1), 810819.

Naser, M., Birst, S. C., 2010. Mesoscopic evacuation modeling for small- to medium-sized metropolitan areas. Tech. rep., Advanced Traffic Analysis Center, Upper Great Plains Transportation Institute, North Dakota State University, Fargo, ND 58108.

Newkirk, R. T., 2001. The increasing cost of disasters in developed countries: A challenge to local planning and government. Journal of Contingencies and Crisis Management 9 (3), 159–170.

NRC, 2006. Facing hazards and disasters: Understanding human dimensions. Tech. rep., National Research Council, Washington, DC: The National Academies Press.

NRC, 2011. Tsunami warning and preparedness: An assessment of the u.s. tsunami program and the nation's preparedness efforts. Committee on the Review of the Tsunami

Warning and Forecast System and Overview of the Nation's Tsunami Preparedness; National Research Council, The National Academies Press.

OSSPAC, 2013. The oregon resilience plan: Reducing risk and improving recovery for the next cascadia earthquake and tsunami. Oregon. Seismic Safety Policy Advisory Commission.

Pan, X., Han, C. S., Dauber, K., Law, K. H., 2007. A multi-agent based framework for the simulation of human and social behaviors during emergency evacuations. Ai & Society 22 (2), 113–132.

Park, H., Cox, D., Lynett, P. J., Wiebe, D. M., Shin, S., 2013. Tsunami inundation modeling in constructed environments: A physical and numerical comparison of free-surface elevation, velocity, and momentum flux. Coastal Engineering 79, 9–21.

Pel, A. J., Bliemer, M. C., , Hoogendoorn, S. P., 2012. A review on travel behaviour modelling in dynamic traffic simulation models for evacuations. Transportation 39 (1), 97–123.

Pel, A. J., Hoogendoorn, S. P., Bliemer, M. C., 2010. Evacuation modeling including traveler information and compliance behavior. Procedia Engineering 3, 101–111.

Pidd, M., de Silva, F. N., Eglese, R. W., 1993. Cemps: a configurable evacuation management and planning systema progress report. Proceedings of the 25th conference on Winter simulation, 1319–1323.

Priest, G. R., Witter, R. C., Zhang, Y. J., 2013. Tsunami animations, time histories, and digital point data for flow depth, elevation, and velocity for the south coast project area, curry county, oregon. Tech. Rep. Open-File Report O-13-13, Department of Geology and Mineral Industries.

Rahimian, S., Mcneil, S., 2012. Post earthquake transportation network performance : Transportation of injured to medical facilities. 2012 NZSEE Conference 59.

Rathi, A. K., Solanki, R. S., 1993. Simulation of traffic flow during emergency evacuations: a microcomputer based modeling system. Proceedings of the 25th conference on Winter simulation, 1250–1258.

Santos, G., Aguirre, B. E., June 2004. A critical review of emergency evacuation simulation models. Nantional Institute of Standards and Technology (NIST) Workshop on Building Occupant Movement during Fire Emergencies.

Satake, K., Wang, K., Atwater, B. F., 2003. Fault slip and seismic moment of the 1700 cascadia earthquake inferred from japanese tsunami descriptions. Journal of Geophysical Research 108 (B11), 1978–2012.

Sheffi, Y., Mahmassani, H., Powell, W. B., 1982. A transportation network evacuation model. Transportation Research Part A: General 16(3), 209–218.

Sheffi, Y., Mahmassani, H. S., Powell, W. B., 1980. Netvac1: A transportation network evacuation model. Center for Transportation Studies, Massachusetts Institute of Technology.

Sherali, H. D., Carter, T. B., Hobeika, A. G., 1991. A location-allocation model and algorithm for evacuation planning under hurricane/flood conditions. Transportation Research Part B: Methodological 25 (6), 439–452.

Sorensen, J. H., 2000. Hazard warning systems: Review of 20 years of progress. Natural Hazards Review 1, 119–125.

Spiess, H., 1990. Conical volume-delay functions. Transportation Science 24 (2).

Thiele, J. C., 2014. R marries netlogo: introduction to the rnetlogo package. Journal of Statistical Software.

Titov, V. V., Gonzalez, F. I., 1997. Implementation and testing of the method of splitting tsunami (most) model. Tech. rep., US Department of Commerce, National Oceanic and Atmospheric Administration, Environmental Research Laboratories, Pacific Marine Environmental Laboratory.

TRB, 2010. Highway Capacity Manual 2010. Transportation Research Board, National Research Council, Washington, D.C.

Tweedie, S. W., Rowland, J. R., Walsh, S. J., Rhoten, R. P., 1986. A methodology for estimating emergency evacuation times. Social Science J. 23 (2), 189–204.

Uno, K., Kashiyama, K., 2008. Development of simulation system for the disaster evacuation based on multi-agent model using gis. Tsinghua Science & Technology 13, 348–353.

Venturato, A. J., Arcas, D., Kanoglu, U., July 2007. Modeling tsunami inundation from a cascadia subduction zone earthquake for long beach and ocean shores, washington. Tech. rep., National Oceanic and Atmospheric Administration, Seattle, WA. Pacific Marine Environmental Lab.

Wang, H., Mostafizi, A., Cramer, L. A., Cox, D., Park, H., 2015. An agent-based modleing of a multimodal near-filed tsunami evacuation: Decission-making and life safety. Trannsportation Reasearch Par C: Emerging Technologies.

Wilensky, U., 1999. Netlogo. http://ccl.northwestern.edu/netlogo/. Center for Connected Learning and Computer-Based Modeling, Northwestern University. Evanston, IL.

Williams, B. M., Tagliaferri, A. P., Meinhold, S. S., Hummer, J. E., Rouphail, N. M., 2007. Simulation and analysis of freeway lane reversal for coastal hurricane evacuation. Journal of urban planning and development 133 (1), 61–72.

Wolshon, B., Urbina, E., Wilmot, C., Levitan, M., 2005. Review of policies and prac-

tices for hurricane evacuation i: Transportation planning, preparedness, and response. Natural Hazards Review 6 (3), 129–142.

Wood, N., 2007. Variations in city exposure and sensitivity to tsunami hazards in oregon. Tech. Rep. 5283, U.S. Geological Survey Scientific Investigations Report.

Wood, N. J., Schmidtlein, M. C., 2012. Anisotropic path modeling to assess pedestrian-evacuation potential from cascadia-related tsunamis in the us pacific northwest. Natural Hazards. 62(2), 275–300.

Wood, N. J., Schmidtlein, M. C., 2013. Community variations in population exposure to near-field tsunami hazards as a function of pedestrian travel time to safety. Natural Hazards. 65 (3), 1603–1628.

Yeh, H., 2010. Gender and age factors in tsunami casualties. Natural Hazards Review 11(1), 29–34.

Zhu, S., Levinson, D., Liu, H. X., Harder, K., 2010. The traffic and behavioral effects of the i-35w mississippi river bridge collapse. Transportation research part A: policy and practice 44 (10), 771–784.

Zhu, S., Levinson, D. M., 2012. Network Reliability in Practice. Springer.